Material Matters™

VOLUME 17 • NUMBER 2

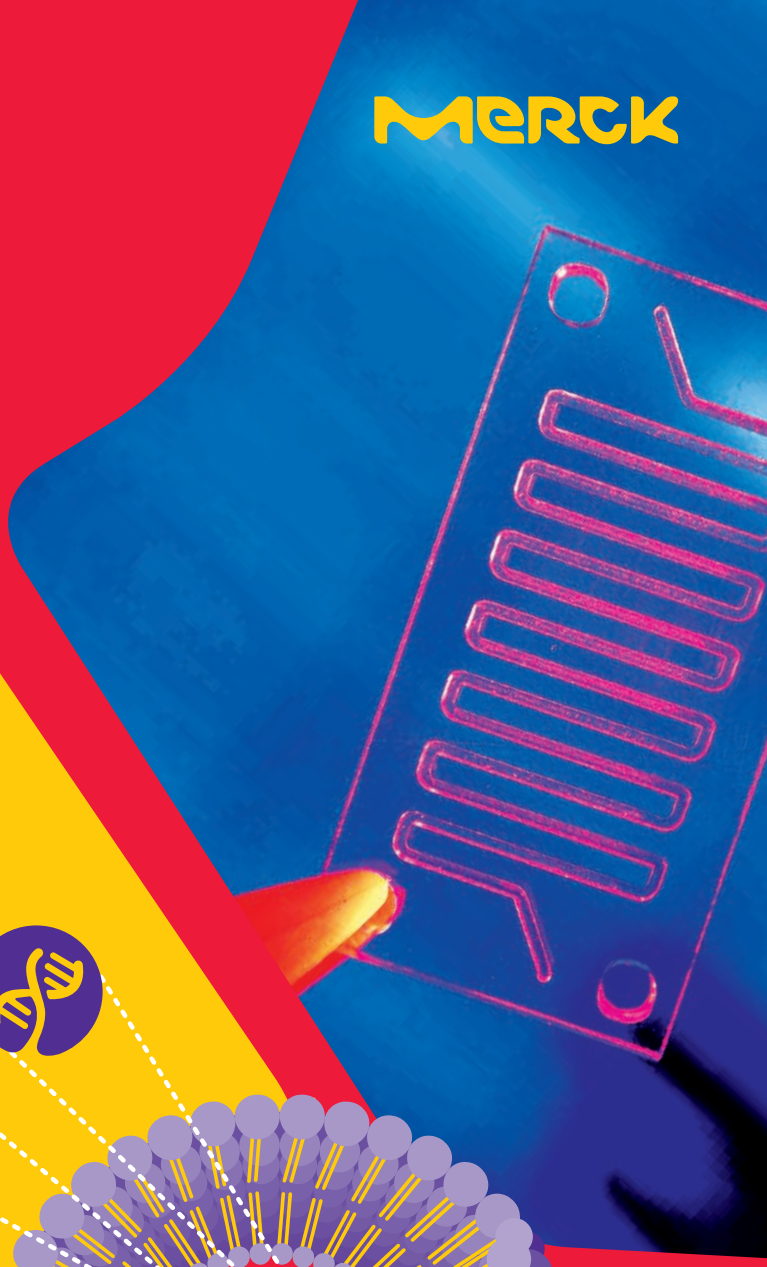

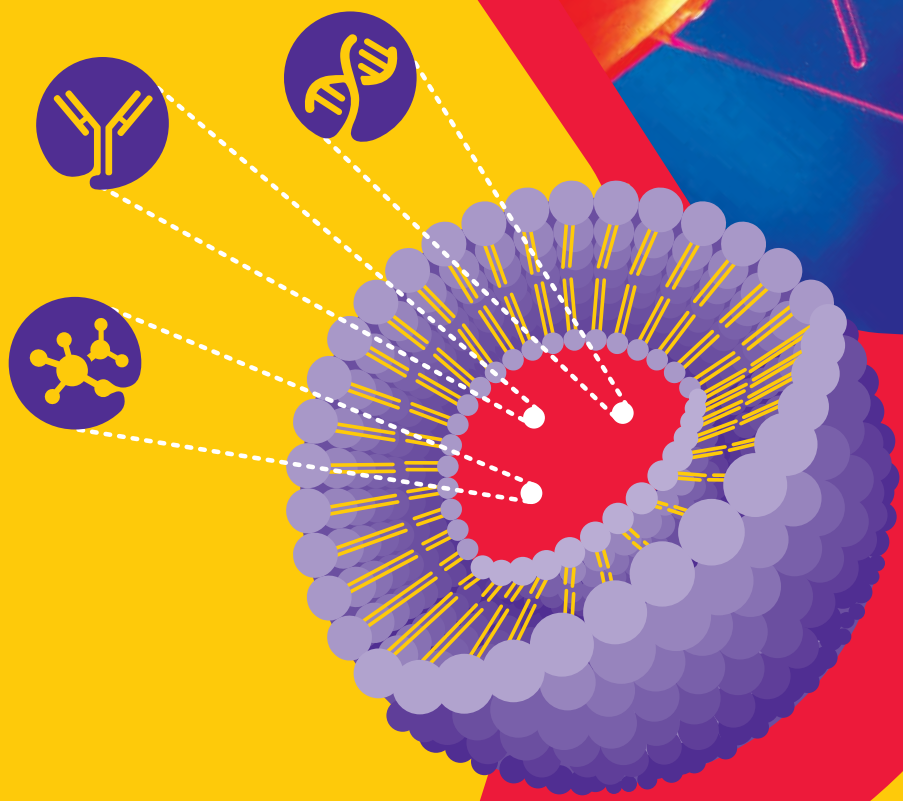

Microfluidics for Nanoencapsulation of Nucleic Acids Using Polymeric Carriers

New Hybridized Multi-Dendrimer Platforms Based on the Supramolecular Assembly Guided by Systematic CNDP Engineering

Polymeric Antioxidants and Nanobiomaterials for Innovative Therapeutic Modalities

Therapeutic Nanoparticles Harness Myeloid Cells for Brain Tumor-targeted Delivery and Immunomodulation

Material Matters™
VOL. 17 • NO. 2

Introduction

Elizabeth Aisenbrey, Ph.D.
Global Product Manager – Biomedical Materials

Welcome to the second issue of Material Matters for 2022, focusing on novel materials and innovative platforms to advance drug delivery. The adoption of nanoparticles for drug delivery can overcome many of the limitations associated with free therapeutics, including improving solubility, navigating biological barriers, and providing controlled and targeted delivery. This issue explores how researchers are tackling existing challenges in the field and offers novel methodologies for improving drug delivery.

In the first article, **Professor Olivia M. Merkel (Ludwig-Maximilians University, Munich, Germany)** introduces microfluidics-based techniques for the encapsulation of nucleic acids in polymeric nanocarriers. Cationic polymers have emerged as promising candidates for nucleic acid delivery due to their flexible and tunable properties. Herein, the application of microfluidics to nucleic acid polyplex fabrication is examined and found to have advantages over conventional procedures by providing precise control, lower polydispersity, and better reproducibility.

Dendrimers offer unique features that are favorable for drug delivery and can be used to bind to drug molecules on the periphery or encapsulate molecules within the dendritic structure. In the second article, **Professor Abhay Singh Chauhan (Medical College of Wisconsin, USA)** describes using well-defined critical nanoscale design parameters (CNDPs) to systematically engineer dendrimers optimized for various applications, including drug delivery. By selecting specific design criteria such as shape, size, and surface chemistry, novel dendrimers with sophisticated nanoelements can be developed for advanced therapeutic applications.

In the third article, **Dr. Ilker S. Bayer (Istituto Italiano di Tecnologia, Italy)** introduces polymeric antioxidants as a new generation of therapeutics to reduce oxidative stress associated with environmental toxicities, cancer, and other stimuli. In addition to improving circulation times and imposing stealth-like properties, polymeric antioxidants can also be used as a multimodal drug delivery vehicle. This review examines the limitations of existing drug delivery carriers and the advantages of polymeric antioxidants.

In the fourth and final article, **Professor Peng Zhang (Northwestern University, USA)** describes the use of therapeutic nanoparticles for brain tumor-targeted delivery. Drug delivery across the blood-brain barrier remains a significant challenge for brain-targeted therapeutics. Here, innovative nanotherapeutic methods harnessing the immunomodulatory effects of tumor-associated myeloid cells (TAMCs) are highlighted, including preferentially hijacking the immune cells as cellular carriers for nanoparticle delivery.

Each article is accompanied by a curated list of related products available from Merck. For more information and additional product offerings, please visit us at SigmaAldrich.com/MatSci. Do you have any new product suggestions or new ideas for future Material Matters™? Please contact us at **SigmaAldrich.com/technicalservice**. We're always happy to hear from you.

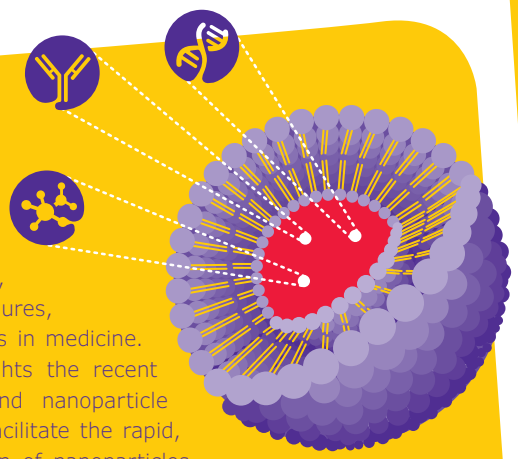

About the Cover

Biomaterials have been an integral part of the exciting new developments in drug delivery. They enable new therapeutic modalities, give new life to diagnostic procedures, and support innovative developments in medicine. The cover art for this issue highlights the recent advancements in drug delivery and nanoparticle synthesis techniques. Microfluidics facilitate the rapid, reproducible, and scalable production of nanoparticles, lipid nanoparticles, and/or liposomes. Prepared lipid nanoparticles (similar to those used for the mRNA Covid vaccine) provide controlled and targeted release of nucleic acids or other therapeutics.

Merck KGaA
Frankfurter Strasse 250
64293 Darmstadt, Germany
Phone +49 6151 72 0

To Place Orders / Customer Service
Contact your local office or visit
SigmaAldrich.com/order

Technical Service
Contact your local office or visit
SigmaAldrich.com/techinfo

General Correspondence
Contact your local office or visit
SigmaAldrich.com/techinfo

Subscriptions
Request your FREE subscription to *Material Matters*™ at **SigmaAldrich.com/mm**

The entire *Material Matters*™ archive is available at **SigmaAldrich.com/mm**

Material Matters™(ISSN 1933-9631) is a publication of Merck KGaA and/or its affiliates

Table of Contents

Articles

Featured Products

Your Material Matters

Nicolynn Davis, Ph.D.
Head of Material Sciences and F&F

Our Drug Delivery Polymers R&D team has recently developed redox-responsive PEG-S-S-PLGA and PEG-S-S-PCL amphiphilic block copolymers (**Cat. Nos. 926248** and **925624**) to further enhance targeted delivery, cellular uptake, and controlled release. These redox-responsive amphiphilic block copolymers contain a reducible disulfide linkage between the hydrophilic poly(ethylene glycol) (PEG) block and the hydrophobic block, poly(lactide-*alt*-glycolide) (PLGA) or poly(caprolactone) (PCL). They can be used to form polymeric micelles or nanoparticles that promote intracellular drug release in response to the surrounding microenvironment.

Redox-responsive nanocarriers have great potential as drug or gene delivery carriers because they can target specific tissue sites and control the release of encapsulated therapeutics. While the disulfide bond is stable in the extracellular environment, upon entering the cell, it undergoes a sulfhydryl-disulfide bond exchange reaction with glutathione (GSH) in the cytoplasm, ultimately cleaving the bond causing the carrier to degrade and release its cargo. Given that GSH levels in tumor cells are far higher than in normal cells, redox-responsive nanocarriers have emerged as a promising platform for tumor-targeted drug delivery.

References

(1) Conte, C.; Mastrotto, F.; Taresco, V.; Tchoryk, A.; Quaglia, F.; Stolnik, Snjezana, Alexander, C. *J. Control. Release* **2018**, *277*, 126–141. https://doi.org/10.1016/j.jconrel.2018.03.011

(2) Li, D.; Zhang, R.; Liu, G.; Kang, Y.; Wu, J. *Adv. Healthc. Mater.* **2020**, *9* (20). https://doi.org/10.1002/adhm.202000605

(3) Fuocco, T.; Pappalardo, D.; Finne-Wistrand, A. *Macromolecules* **2017**, *50* (18), 7052–7061. https://doi.org/10.1021/acs.macromol.7b01318

Name	Cat. No.
Redox Responsive Poly(ethylene glycol)-*block*-poly(lactide-*alt*-glycolide), PEG average M_n 5,000, PCL M_n 15,000	**926248-1G**
Redox Responsive Poly(ethylene glycol)-*block*-poly (ε-caprolactone), PEG average M_n 5,000, PCL M_n 15,000	**925624-1G**

Product Highlight

Formulation Made Easier

NanoFabTx™ Formulation Kits

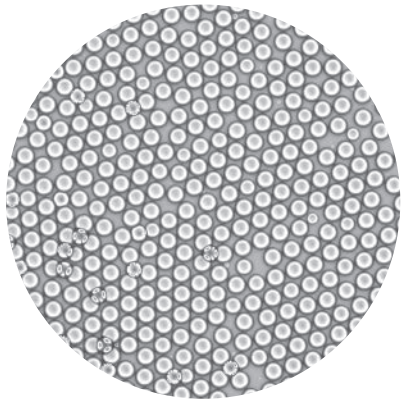

Formulate faster with our ready-to-use NanoFabTx™ formulation kits. NanoFabTx™ kits facilitate early-stage drug nanoformulation screening with optimized protocols and a curated selection of polymer- and lipid-based materials for drug encapsulation.

Key Features:

- Step-by-step protocols developed by our formulation scientists
- Flexible synthesis tool optimized to create uniform and reproducible 100–200 nm nanoparticles or 1–30 µm microparticles such as:
  - **911593** NanoFabTx™ microfluidic - nano, device kit for synthesis of 100–200 nm nanoparticles and liposomes
  - **911860** NanoFabTx™ microfluidic - micro, device kit for synthestsis of 1–5 µm particles
- Protocols allow a choice of standard glassware-based nanoprecipitation or microfluidic-based preparation
- Material screening kits available, like:
  - **915408** NanoFabTx™ PEGylated nanoparticle formulation screening kit

Explore our products:
SigmaAldrich.com/nanofabtx

Microfluidics for Nanoencapsulation of Nucleic Acids Using Polymeric Carriers


Friederike Adams[1,2*] and Olivia M. Merkel[3]

[1] Chair of Macromolecular Materials and Fiber Chemistry, Institute of Polymer Chemistry, University of Stuttgart, Pfaffenwaldring 55, 70569 Stuttgart, Germany
[2] Institute for Ophthalmic Research, University Eye Hospital Tübingen, Elfriede-Aulhorn-Strasse 7, 72076 Tübingen, Germany
[3] Department of Pharmacy, Pharmaceutical Technology and Biopharmacy, Ludwig-Maximilians University Munich, 81377 Munich, Germany
* Email: friederike.adams@ipoc.uni-stuttgart.de

Introduction

In contrast to lipid nanoparticles (LNPs), which are commonly actively loaded with nucleic acids, polycations such as polyamines self-assemble with polyanionic nucleic acids into so-called polyelectrolyte complexes (short polyplexes) due to electrostatic attraction. Their disadvantage compared to LNPs, is their less defined morphology and composition, which has been reported to lead to polydisperse particle size distribution and poorly reproducible formulations.[1] By microfluidic assembly of nucleic acid/carrier complexes, both disadvantages can be addressed efficiently for formulating defined and reproducible RNA nanocarriers.[2] For more information on microfluidics for the preparation of LNPs, we recommend Reference 3. Amongst polyamines used for complexation, polyethylenimine (PEI) and poly-l-lysine (PLL), as well as their derivatives, are most widely used for preclinical applications. Additionally, polyamidoamine (PAMAM) dendrimers, poly(2-(dimethylamino)ethyl methacrylate (PDMAEMA), or polyamines of natural origin, such as chitosan, cationic gelatin or pullulan, and arginine-rich peptides have been described for polyplex formation.[4] Polyamines, which have been chosen in various studies for microfluidic assembly of nucleic acid polyplexes, are depicted in **Figure 1**.

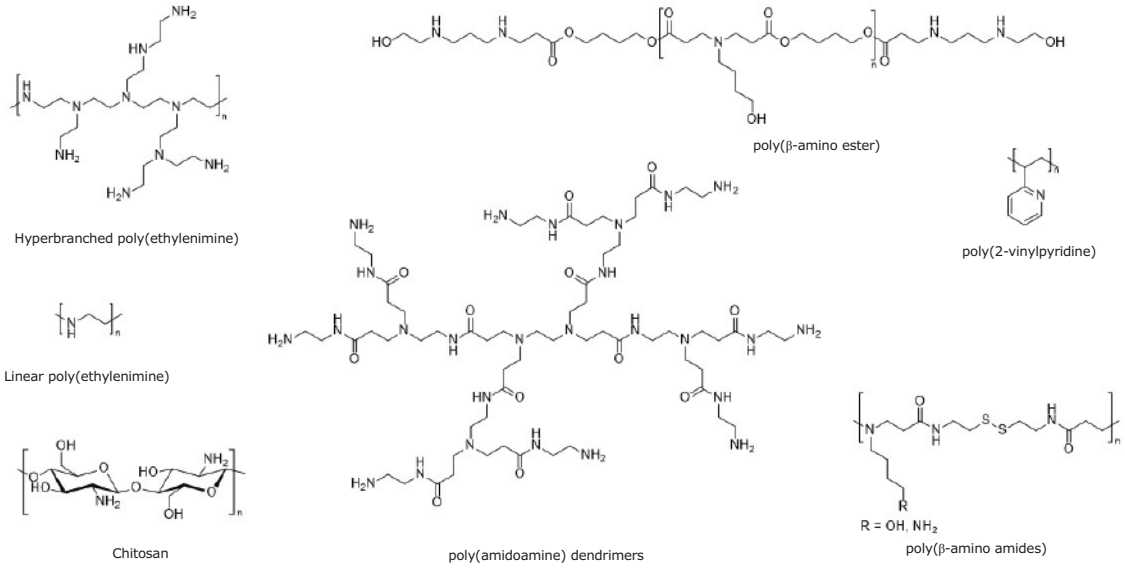

Figure 1. Cationic polymeric carriers used for microfluidic mixing with nucleic acids. For poly(amidoamine) (PAMAM) dendrimers, PAMAM generation 2 is shown. For more information on PAMAM dendrimers, we refer to Reference 5.

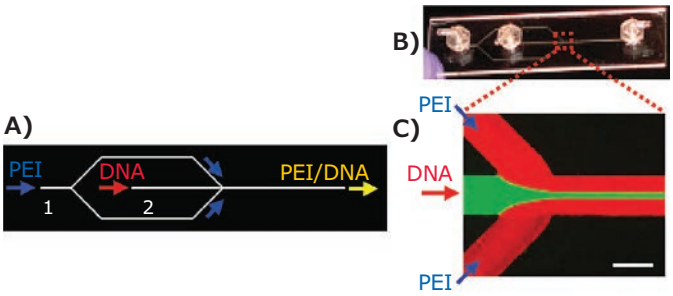

Figure 2. A and B) Microfluidic hydrodynamic focusing device with two inlets and one outlet for the preparation of pDNA/PEI complexes. C) Fluorescence micrograph of the flow pattern using fluorescein dye and Rhodamine-labeled PEI. Reproduced with permission from reference 6, copyright 2009, American Chemical Society.

Microfluidic Mixing Using Flow Focusing

The first microfluidic systems with cationic carriers for encapsulating nucleic acids were used in 2009 to encapsulate plasmid DNA (pDNA) in 25 kg/mol hyperbranched PEI. Microfluidic mixing was performed to prevent large particle size distributions of DNA/PEI complexes caused by conventional bulk mixing and to improve general particle characteristics, cell viabilities, and transgene expression. A simple poly(methyl methacrylate) microfluidic hydrodynamic focusing device (MF) was used at flow rates of 10 and 50 µL/min for the middle (DNA solution) or side channels (PEI solution), respectively. The DNA stream was hydrodynamically focused into a narrowly focused stream by the two PEI side streams **(Figure 2)**.[6]

A similar simple microfluidic device was used to study the DNA polyplex self-assembly under laminar flow in real time using quantum-dot mediated fluorescence resonance energy transfer (QD-FRET) studies. pDNA was labeled with quantum dots as the FRET-donor, and Cy5-dye-conjugated chitosan was used as the biodegradable, non-toxic, cationic carrier and FRET acceptor. Due to the preservation of a laminar flow after combining both solutions in a T-junction, mixing solely took place at the interface of both streams enabling precise self-assembly kinetics monitored by FRET. Detection of Cy5 emission confirmed successful DNA/chitosan polyplex formation. Emission was detected right after combining both flows in the T-junction, showing immediate DNA/carrier interactions with increasing polyplex concentrations over time.[7]

Three-dimensional hydrodynamic flow focusing was chosen by Quinones-Hinojosa et al. to produce poly(β-amino ester)/DNA polyplexes. The continuous flow assembly of these polyplexes was performed at a rate of 100 mg/h using a high flow rate of 45 ml/h. To overcome problems of long-term storage of polyplexes or polyesters in aqueous solutions, nanocomplexes were lyophilized. After three months of storage at -20 °C, these particles showed similar transfection efficiencies in glioblastoma cells. Still, in melanoma and breast cancer cells, transgene expression was only comparable to freshly prepared polyplexes when the particles were prepared using microfluidics. By nanoparticle tracking analysis of polyplexes loaded with Cy3-labeled plasmids, the authors attempted to determine nanoparticle concentration and the number of plasmids per particle.[8]

Microfluidic Mixing Chips with Loops

To increase interactions between polymers and nucleic acid solutions in the microfluidic channels, active mixers are equipped with baffles that induce controlled turbulent flow rather than laminar flow. In one example, Kissel et al. investigated the formation of PEI/pDNA polyplexes using a microfluidic device and polyplexes with modified PEI (hyperbranched, 25 kg/mol and 5 kg/mol) and siRNA or mRNA as nucleic acids. Polyplexes were prepared in a microfluidic lab-on-a-chip assembly using different flow rates. PEI and nucleic acid solutions were pumped separately into a mixing chip composed of different geometries with varying mixing lengths and designs. Mixing behaviors in the different chips were evaluated with trypan blue and 5(6)-carboxyfluorescein solutions under a microscope. As some designs showed a laminar flow of both solutions even after traversing the Y-junction without any subsequent mixing, a loop was necessary following the Y-part to facilitate the mixing of PEI and DNA to form small and uniform polyplexes. The particle sizes of PEI/pDNA polyplexes mainly depended on the ratio between the cationic carrier and nucleic acid (N/P ratio) with uniform sizes at N/P = 5–20 and independent from concentrations or flow rates.[9] Further odn, the group used a lower-molecular weight fraction of 25 kg/mol PEI, 5kg/mol PEI and Transferrin-PEI (5 kg/mol) for specific targeting approaches in combination with pDNA, siRNA, and mRNA. For pDNA, polyplex sizes were similar regardless of the preparation method, but polydispersities were lower for microfluidic mixing compared to pipetting. The same microfluidic mixing method was transferable to other nucleic acids since similar sized polyplexes with these polymers and siRNA or mRNA were formed; generally, higher polydispersities were observed when using siRNA.[9]

The groups of Kissel and Merkel evaluated a more sophisticated PEI copolymer. An amphiphilic water-insoluble triblock copolymer consisting of a hydrophilic poly(ethylene glycol), hydrophobic poly(caprolactone), and 2.5 kg/mol linear PEI (PEG-PCL-PEI) was used as an siRNA carrier.[10] Microfluidic mixing led to the smallest, most uniform, and most stable particles compared to all other tested techniques when using a solution of pre-formed nanocarrier prepared via solvent-displacement technique and a nucleic acid solution using the same microfluidic setup that was most efficient in their previous study (vide supra). In addition, slightly higher transfection efficiencies were observed in SKOV3 cells for these polyplexes, in which the knockdown was increased from 24.5% (polyplexes via pipetting) to 34.8%.[10] Merkel et al. further developed these studies using a water-soluble

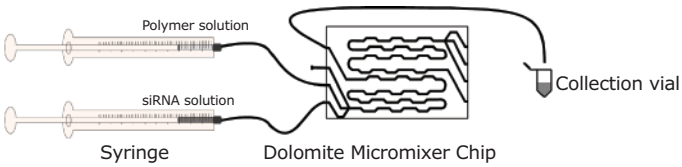

Figure 3. Schematic drawing of microfluidic mixing of PEI and siRNA using a Dolomite Micromixer Chip. Reproduced with permission from reference 2, copyright 2017, IOP Publishing.

PEG-PCL-PEI polymer of hyperbranched 25 kg/mol PEI. A Dolomite micromixer chip was used in which a polymer and an siRNA solution were individually pumped into the chip with a flow rate of 0.5 mL/min (**Figure 3**). At this lowest flow rate of the three tested ones, polyplexes were only half the size of those prepared by bulk mixing with a narrower size distribution. While the smaller size did not result in any benefits regarding *in vitro* transfection, it was clearly shown that these polyplexes were more efficiently taken up in the lung parenchyma after intratracheal *in vivo* administration, which was discussed as a result of less efficient clearance by macrophages in the lung.[2] The same group showed that this setup efficiently sensitized lung cancer cells to cisplatin using siRNA targeted to ERCC1 and XPF. After downregulating two of the most efficient pathways that repair platinum-induced DNA damage by 80–90% in p53 wildtype lung cancer cells, their IC_{50} sensitivity toward cisplatin was decreased by factor 2.[11]

A more complex system in which cationic 2.5 kg/mol PEI-β-cyclodextrin (PEI-CD), hyaluronic acid-adamantane (HA-Ad), and pDNA were mixed in a commercial Chemtrix microreactor was developed by Thompson et al. using a layer-by-layer approach (**Figure 4**). PEI-CD and pDNA were assembled through two inlets at N/P ratios of 10, 20, or 30 and pDNA flow rates of 5, 10, or 20 µL/min. After self-assembly, HA-Ad was added in a separate inlet at the end of the mixing chip. HA-Ad was used due to its water solubility, CD44 targeting capability, and biocompatibility to serve as a protective shell. Higher flow rates led to smaller particles with narrower size distributions and lower Zeta-potentials compared to a similar bulk mixing procedure. However, polyplex stability studies with PicoGreen indicated that polyplexes prepared by flow mixing were less stable in the presence of heparin as a competing polyanion and more susceptible to disassembly. The reduced stability in combination with reduced Zeta-potentials was hypothesized to cause decreased transfection efficacies for flow-mixed complexes on the one hand with decreased cytotoxicity on the other hand.[12]

In a similar two-step approach, Moffitt et al. studied the self-assembly of cationic poly(2-vinylpyridine)-*block*-poly(ε-caprolactone) (P2VP-PCL) with pDNA, followed by a second assembly with micellar poly(ethylene glycol)-*block*-poly(ε-caprolactone) (PEG-PCL) resulting in "polyplex-in-hydrophobic

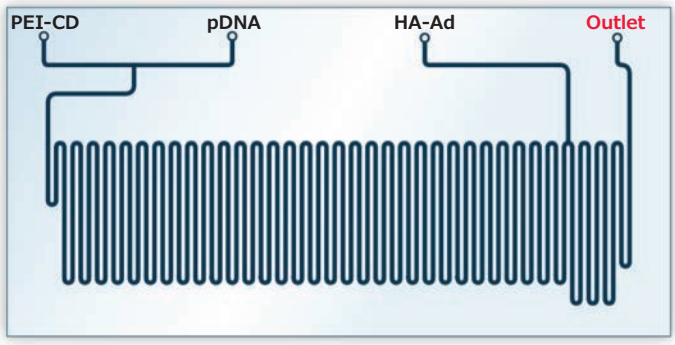

Figure 4. Chemtrix microreactor (Design 3023) with three inlets and one outlet for the formation of PEI-CD, pDNA polyplexes that are further assembled with HA-Ad. Reprinted with permission from reference 14, copyright 2022 Chemtrix BV.

core" (PIHC) micelles. The microfluidic technique was solely used for the second assembly step to control the mixing of water and dioxane with a solution of the previously assembled P2VP-PCL/pDNA polyplex already combined with the PEG-PCL polymer.[13]

Other Microfluidic Micromixer

Polyplexes with a 22 kg/mol linear PEI and pDNA were prepared with a micro-mixer at different speeds to investigate the impact of mixing speed on the polyplex characteristics. The up-scaled micromixer was composed of two syringe pumps pumping the PEI- and DNA-solution into a conventional T-shape connection, commonly used as a connector in HPLC analysis. Different speeds and plasmid concentrations were set to investigate the influence on polyplex formation. An increasing rate of mixing and a decrease in DNA concentration led to decreased and reproducible particle sizes (down to 50 nm) and exceptionally low polydispersities of 0.05. However, metabolic and transfection activities *in vitro* showed no differences between polyplexes prepared via up-scaled micro-mixing or more heterogeneous particles prepared by pipetting at a large volume.[15]

A more complex setup was investigated by Foged et al. in which three inlets were connected to a micromixer. One syringe with siRNA solution in the center inlet and two syringes with generation 4 PAMAM dendrimer in the outer inlets were pumped into a 3D printed micromixer to form polyplexes. The tailor-made micromixer was designed according to the desired flow pattern after performing simulation studies. Testing different flow rates, increased flow rates led to smaller particles. However, these sizes and polydispersities were not improved compared to bulk mixing at an N/P ratio of 20. Afterward, these polyplexes were transferred into microparticle-based powders via spray drying for inhalation therapy. Different saccharides were used during the spray drying process to obtain nanoembedded-microparticles (NEM). Several nanocomplex-to-matrix (N/M) ratios were tested

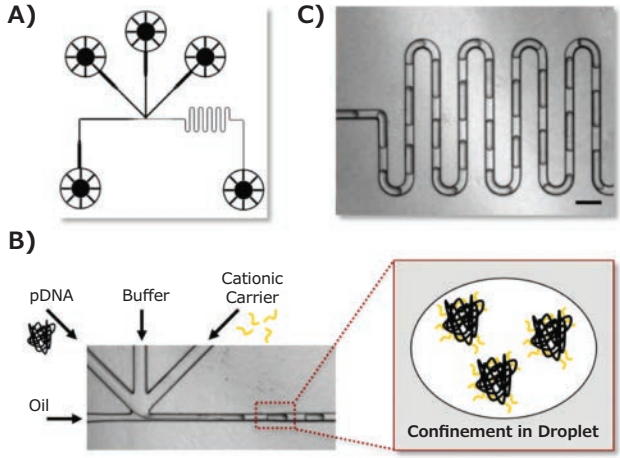

Figure 5. Microfluidic assembly of pDNA polyplexes in picolitre droplets using a crossflow type droplet generator. Reproduced with permission from reference 17, copyright 2011, American Chemical Society.

with all excipients. Spheric particles with aerodynamic particle diameters of 5 µm with residual moisture contents between 0.2 (for mannitol) and 6 wt.% (for trehalose) were obtained. The viability of RAW264.7 cells was only slightly affected by the nanocomplexes at siRNA concentrations up to 400 nM. Cell uptake of NEM in the same cell line was verified via confocal microscopy using fluorescent siRNA and flow cytometry showing the highest cellular uptake for NEMs with a trehalose/inulin mixture of 50/50. Furthermore, this NEM induced an 87% inhibition of TNF-α expression in gene silencing experiments which was in the same range as freshly prepared nanocomplexes without excipient. The specific impact of microfluidic mixing alone on transfection efficacy was not investigated in this study.[16]

Droplet-based Approaches

By using the commercially available transfection agents jetPEI®, which is a 20 kg/mol linear polyethylenimine derivative, or Turbofect (poly(2-hydroxypropylenimine)) and pDNA in microfluidics-assisted confinement (MAC), Leong et al. were able to produce picolitre droplets consisting of well-defined nanocomplexes. The droplets were produced in a crossflow microfluidic droplet generator via competing flows of the continuous oil phase and disperse aqueous phase. Plasmid DNA, PEI, and buffer solutions were injected into an individual channel each via syringe pumps. DNA and carrier solutions were confined into individual droplets and were mixed in a serpentine channel to form nanocomplexes via electrostatic interactions (**Figure 5**). Buffer solution was used to avoid aggregation. Polyplexes formed via this method showed more monodisperse diameters with slightly more neutral Zeta-potentials and an increased nanocomplex stability compared to bulk mixing indicating optimal encapsulation of pDNA and resistance to aggregation. After incubation with HEK293 cells, polyplexes formed via microfluidics showed increased cell viability for both polymers and slightly better transfection when using Turbofect. It was shown that larger polyplexes resulting from bulk mixing partially showed higher uptake efficacies at early time points but leveled off. In contrast, smaller and more stable MAC-produced particles had a more consistent uptake.[17] This observation is perfectly in line with the hypothesis that larger bulk particles sediment faster and may therefore result in efficient uptake,[2] particularly at early time points,[17] masking potential benefits of microfluidic mixing.[15]

The same group investigated the self-assembly of bioreducible poly(amido amines) with pDNA or mRNA in the same microfluidic device. Improved nanoparticle characteristics (smaller, more uniform, less aggregation) were observed. QD-FRET and flow cytometry were used to quantify the intracellular unpacking of polyplexes and DNA release. DNA-polyplexes produced by MAC showed increased colloidal and binding stability, and transfection was improved in various cell lines (HEK293, primary mouse embryonic fibroblasts, human mesenchymal stem cells, and HepG2 human hepatocellular carcinoma cells). These higher efficiencies were caused by more gradual release of the payload as monitored by QD-FRET.[18]

Chen et al. designed a similar droplet-based microfluidic device coupled to a dielectrophoresis (DEP) setup to directly sort polymer/pDNA nanocomplexes from the oil phase in a non-uniform electric field. As a cationic carrier, low molecular weight fatty acid-cyclodextrin-PEI (600 g/mol) was used, which already showed high transfection efficiency and low cytotoxicity in previous studies. DEP further decreased polydispersity and sizes of polyplexes compared to batch mixing/pipetting and on-chip mixing without DEP. Transfection efficacy, claimed to be increased by DEP mixing, was only assessed by microscopic counting of fluorescent cells, but no quantitative results were presented.[19]

Conclusion

Microfluidic mixing allows for controlled assembly of nucleic acid polyplexes, which in several accounts was reported to have beneficial effects on polyplex size and polydispersity. Regarding efficacy, the picture is not clear, which could result from most studies investigating only *in vitro* transfection. As pointed out, uptake kinetics depend on particle size in typical two-dimensional cell culture setups. Larger particles that sediment faster could mask potential benefits that smaller particles offer in the long run. In an *in vivo* study, clearance of larger particles by phagocytosing cells plays a more significant role; therefore, differences can be shown more clearly. Overall, microfluidic mixing conditions must be optimized for each mixing system and may also be affected by the materials and solvents used. The most significant advantage, however, is the ability to reproduce and scale up the production process.

Acknowledgment

F.A. is grateful for funding from the Federal Ministry of Education and Research (BMBF) and the Baden-Württemberg Ministry of Science, Research and Art as part of the Excellence Strategy of the German Federal and State Governments. O.M.M. acknowledges support from the European Research Council (ERC-2014-StG – 637830), from the Bavarian Research Foundation (AZ-1449-20C) and from the Center for NanoScience at LMU Munich.

References

(1) Kozielski, K. L.; Tzeng, S. Y.; Hurtado De Mendoza, B. A.; Green, J. J. *ACS Nano* **2014**, *8* (4), 3232–3241.
(2) Feldmann, D. P.; Xie, Y.; Jones, S. K.; Yu, D.; Moszczynska, A.; Merkel, O. M. *Nanotechnology* **2017**, *28* (22), 224001.
(3) Ali, M. S.; Hooshmand, N.; El-Sayed, M.; Labouta, H. I. *ACS Appl. Bio Mater.* **2021**, DOI: 10.1021/acsabm.1c00732.
(4) Merkel, O. M.; Kissel, T., J. *Control. Release* **2014**, *190*, 415–23.
(5) Boas, U.; Christensen, J. B.; Heegaard, P. M. H. *J. Mater. Chem.* **2006**, *16* (38), 3785–3798.
(6) Koh, C. G.; Kang, X.; Xie, Y.; Fei, Z.; Guan, J.; Yu, B.; Zhang, X.; Lee, L. J. *Mol. Pharm.* **2009**, *6* (5), 1333–1342.
(7) Ho, Y.-P.; Chen, H. H.; Leong, K. W.; Wang, T.-H. *Nanotechnology* **2009**, *20* (9), 095103.
(8) Wilson, D. R.; Mosenia, A.; Suprenant, M. P.; Upadhya, R.; Routkevitch, D.; Meyer, R. A.; Quinones-Hinojosa, A.; Green, J. J. *J. Biomed. Mater. Res. A* **2017**, *105* (6), 1813–1825.
(9) Debus, H.; Beck-Broichsitter, M.; Kissel, T. *Lab Chip* **2012**, *12* (14), 2498–2506.
(10) Endres, T.; Zheng, M.; Beck-Broichsitter, M.; Samsonova, O.; Debus, H.; Kissel, T. *J. Control. Release* **2012**, *160* (3), 583–591.
(11) Feldmann, D. P.; Heyza, J.; Zimmermann, C. M.; Patrick, S. M.; Merkel, O. M. *Molecules* **2020**, *25* (8), 1994.
(12) Kulkarni, A.; VerHeul, R.; DeFrees, K.; Collins, C. J.; Schuldt, R. A.; Vlahu, A.; Thompson, D. H. *Biomater. Sci.* **2013**, *1* (10), 1029–1033.
(13) Kly, S.; Andrew, L. J.; Moloney, E. G.; Huang, Y.; Wulff, J. E.; Moffitt, M. G. *Chem. Mater.* **2021**, *33* (17), 6860–6875.
(14) Chemtrix Labtrix - Flow Chemistry Method Development. https://siteassets.pagecloud.com/proteaf/downloads/Brochure_Labrix-ID-0b4b0a25-f2ab-4c40-8637-1ec275be4897.pdf.
(15) Kasper, J. C.; Schaffert, D.; Ogris, M.; Wagner, E.; Friess, W. *Eur. J. Pharm. Biopharm.* **2011**, *77* (1), 182–185.
(16) Agnoletti, M.; Bohr, A.; Thanki, K.; Wan, F.; Zeng, X.; Boetker, J. P.; Yang, M.; Foged, C. *Eur. J. Pharm. Biopharm.* **2017**, *120*, 9–21.
(17) Ho, Y.-P.; Grigsby, C. L.; Zhao, F.; Leong, K. W. *Nano Lett.* **2011**, *11* (5), 2178–2182.
(18) Grigsby, C. L.; Ho, Y.-P.; Lin, C.; Engbersen, J. F. J.; Leong, K. W. *Sci. Rep.* **2013**, *3* (1), 3155.
(19) Yang, S.-M.; Yao, H.; Zhang, D.; Li, W. J.; Kung, H.-F.; Chen, S.-C. *Microfluid. Nanofluidics* **2015**, *19* (1), 235–243.

Poly(ethyleneimine) (PEI) for Gene Delivery

Name	Molecular Weight	Description	Cat. No.
Poly(ethyleneimine) solution	average M_n ~1,200 average M_w ~1300 by LS"	50 wt. % in H_2O	**482595-100ML** **482595-250ML**
	average M_n ~1,800 by GPC average M_w ~2,000 by LS	50 wt. % in H_2O	**408700-5ML** **408700-250ML** **408700-1L**
	average M_n ~60,000 by GPC average M_w ~750,000 by LS	50 wt. % in H_2O	**181978-5G** **181978-100G** **181978-250G**
Polyethylenimine hydrochloride	average M_n 4,000	PDI ≤1.3	**764892-1G** **764892-5G**
	average M_n 10,000	PDI ≤1.5	**764647-1G**
	average M_n 20,000	PDI ≤1.4	**764965-1G**
Polyethylenimine, 80% ethoxylated solution	M_w 110,000	37 wt. % in H_2O	**306185-100G** **306185-250G**
Polyethylenimine, branched	average M_n ~600 by GPC average M_w ~800 by LS		**408719-100ML** **408719-250ML** **408719-1L**
	average M_n ~10,000 by GPC average M_w ~25,000 by LS		**408727-100ML** **408727-250ML** **408727-1L**
Polyethylenimine, linear	average M_n 2,100	PDI <1.3	**764604-1G**
	average M_n 5,000	PDI ≤1.3	**764582-1G**
	average M_n 10,000	PDI ≤1.3	**765090-1G**

Chitosan for Gene Delivery

Name	Description	Form	Cat. No.
Chitosan	low molecular weight	powder	**448869-50G** **448869-250G**
	medium molecular weight	powder	**448877-50G** **448877-250G**
	high molecular weight	coarse ground flakes and powder	**419419-50G** **419419-250G**
Trimethyl chitosan	low molecular weight, degree of quaternization >50%	powder	**912700-1G**
	medium molecular weight, degree of quaternization: 40-60%	powder	**912123-1G**
	high molecular weight, degree of quaternization >70%	powder	**912034-1G**

Microfluidic Mixing Chips and Droplet Generators

Name	Description	Cat. No.
Diffusion mixer chip	Fluidic 186, COP	**926353-1EA**
	Fluidic 186, PC	**926361-1EA**
Droplet generation and storage chip	Fluidic 488, COC	**921661-1EA**
	Fluidic 488, PC	**921688-1EA**
	Fluidic 719, COC	**921513-1EA**
	Fluidic 719, PC	**921483-1EA**
Droplet generator chip - Droplet size variation	Fluidic 947, COC	**922021-1EA**
Droplet generator chip - Four elements per chip design	Fluidic 537, COC	**922005-1EA**
	Fluidic 537, PC	**922013-1EA**
Droplet generator chip - Multi channel design	Fluidic 1032, COC	**921653-1EA**
	Fluidic 1032, PC	**921998-1EA**
	Fluidic 285, COC	**921955-1EA**
	Fluidic 285, PC	**921963-1EA**
	Fluidic 440, COC	**921394-1EA**
	Fluidic 440, PC	**921505-1EA**
	Fluidic 912, COC	**921971-1EA**
	Fluidic 912, PC	**921718-1EA**
Droplet generator chip - One channel design	Fluidic 162, COC	**921424-1EA**
	Fluidic 162, PC	**921491-1EA**
	Fluidic 163, COC	**921645-1EA**
	Fluidic 163, PC	**921696-1EA**
Droplet Generator Chip With Monitoring Chamber	Fluidic 1114, COC	**928488-1EA**
	Fluidic 1114, PC	**928461-1EA**
	Fluidic 1147, COC	**928453-1EA**
	Fluidic 1147, PC	**928445-1EA**
Finger Pump Mixer Chip	Fluidic 999, COC	**926477-1EA**
	Fluidic 999, COP	**926434-1EA**
Herringbone Mixer Chip	Fluidic 187, COP	**926493-1EA**
	Fluidic 187, PC	**926507-1EA**
Micro Vortex Mixer Chip	Fluidic 641, COC	**926337-1EA**
	Fluidic 641, PC	**926264-1EA**
	Fluidic 641, PMMA	**926329-1EA**
	Fluidic 642, COC	**926256-1EA**
	Fluidic 642, PC	**926299-1EA**
Pearl-chain mixer	Fluidic 658, COC	**921807-1EA**
	Fluidic 658, PC	**921815-1EA**
Phase Guide Mixer Chip	Fluidic 533, COC	**926485-1EA**
Snowman Mixer Chip	Fluidic 1108, COC	**926302-1EA**
Stir Bar Actuated Mixer Chip	Fluidic 286, COP	**926272-1EA**
	Fluidic 286, PMMA	**926280-1EA**

NanoFabTx™ Microfluidic Device Kits

Name	Description	Kit Components	Cat. No.
NanoFabTxTM microfluidic - nano	device kit for synthesis of 100-200 nm nanoparticles and liposomes	Microfluidic chip x 1 Tubings and accessories	**911593-1EA**
NanoFabTxTM microfluidic - micro	device kit for synthesis of 1-5 µm particles	Microfluidic chip x 1 Tubings and accessories	**911860-1EA**
NanoFabTxTM microfluidic - micro	device kit for synthesis of 10-30 µm particles	Microfluidic chip x 1 Tubings and accessories	**911879-1EA**

NanoFormulation On-a-Chip

Microfluidic solutions for nanoparticle synthesis

Shrink your lab to micro-scale and improve your nanoparticle synthesis with our microfluidic chips.

We offer a wide range of products including:

- Mixer chips
- Droplet generator chips
- Reaction chamber chips
- And more!

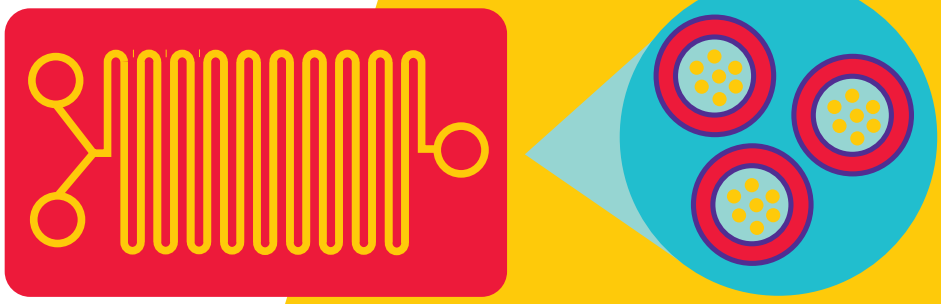

To explore the entire catalog, please visit:
SigmaAldrich.com/microfluidic-chip

43540 08/2022

The Life Science business of Merck operates as MilliporeSigma in the U.S. and Canada.

Sigma-Aldrich®
Lab & Production Materials

New Hybridized Multi-Dendrimer Platforms Based on the Supramolecular Assembly Guided by Systematic CNDP Engineering



Mayank Kumar Singh,[1] Donald Andrew Tomalia,[1,2,3] Abhay Singh Chauhan,[4,5*]

[1] The National Dendrimer & Nanotechnology Center, NanoSynthons LLC, Mount Pleasant, Michigan 48858, United States
[2] Department of Chemistry, University of Pennsylvania, Philadelphia, Pennsylvania 19104, United States
[3] Department of Physics, Virginia Commonwealth University, Richmond, Virginia 23287, United States
[4] Department of Biopharmaceutical Sciences, Medical College of Wisconsin-School of Pharmacy, Milwaukee, Wisconsin 53226, United States
[5] Amruth LLC, Milwaukee, Wisconsin 53226, United States
[*] Email: achauhan@mcw.edu

Introduction

In 1979, while working in Dow Chemical Company Research Laboratory, D. A. Tomalia et al. discovered a homologous series of 3-dimensional, hyperbranched macromolecules that appeared to mimic "tree branching". This fourth new class of polymer architecture both stunned and synergized the polymer world when it was first reported at a Winter Gordon Conference (1983), followed by several peer-reviewed publications (1984–86),[1-4] and later in patents (U.S. Patent 4,507,466, Tomalia and Dewald, 1985). Synthesis of these unprecedented hyperbranched polymers began with a defined atomic or molecular initiator core. It involved a divergent, geometrically driven growth process that produced concentric layers of covalently branched poly(amido) amine (PAMAM) moieties around the core, much like the layers of an onion (**Figure 1**). These concentric PAMAM layers were reminiscent of annual growth rings found in trees (i.e., "dendrochronology") and prompted Tomalia to refer to these new polymeric architectures as *dendrimers*. This new term was derived from the Greek word "*dendri*" for branched and the word *"mer"*, meaning "part of".

Dendrimers are precise, mathematically defined, covalent hyperbranched, macromolecular nanostructures. As such, their interiors are composed of quantized numbers of covalently bound monomers, whereas precise numbers of terminal functional groups reside on their surfaces as a function of the respective layers (i.e., generations) that surround the core (**Figure 2**). Historically, these Tomalia-type PAMAM dendrimers are recognized as the first dendrimer family to be synthesized and become commercially available with surface groups, as shown in **Figure 3**.

Currently, dendrimers may be found in many commercial applications, including targeted cancer therapy (DEP® docetaxel, Starpharma), anti-microbicidal activity against HIV and HSV (VivaGel®, Starpharma), antiviral nasal spray to protect against SARS-CoV-2 (VIRALEZE™ Starpharma), controlled delivery of herbicides (Priostar® dendrimers, Agrium/Nutrien agrochemicals) and the measurement of cardiac markers (i.e., Troponin, Stratus® CS, Siemens) are just a few commercial dendrimer-based products to be mentioned. A more complete list of commercialized dendrimer-based formulations is summarized elsewhere by Chauhan et al.[7]

Next, we overview certain key intrinsic dendrimer features that may be systematically engineered to produce unique multi-dendrimer nano-devices that clearly differentiate dendritic systems from all other nanoscale structures.

A Systematic Framework for Unifying and Defining Dendrimer Structures

The dendrimer-based nanotechnology movement is a multidisciplinary area navigated by many traditional disciplines, including chemistry, physics, biology, mathematics, medicine, pharmacology, advanced materials, engineering, toxicology, and environmental sciences. Many of these important dendrimeric structures have been synthesized and optimized for specific performance/application objective by manipulating six well-defined intrinsic features referred to as "critical nanoscale design parameters" (CNDPs), which includes: (1) architecture, (2) elemental composition, (3) flexibility/rigidity, (4) shape, (5) size, and (6)

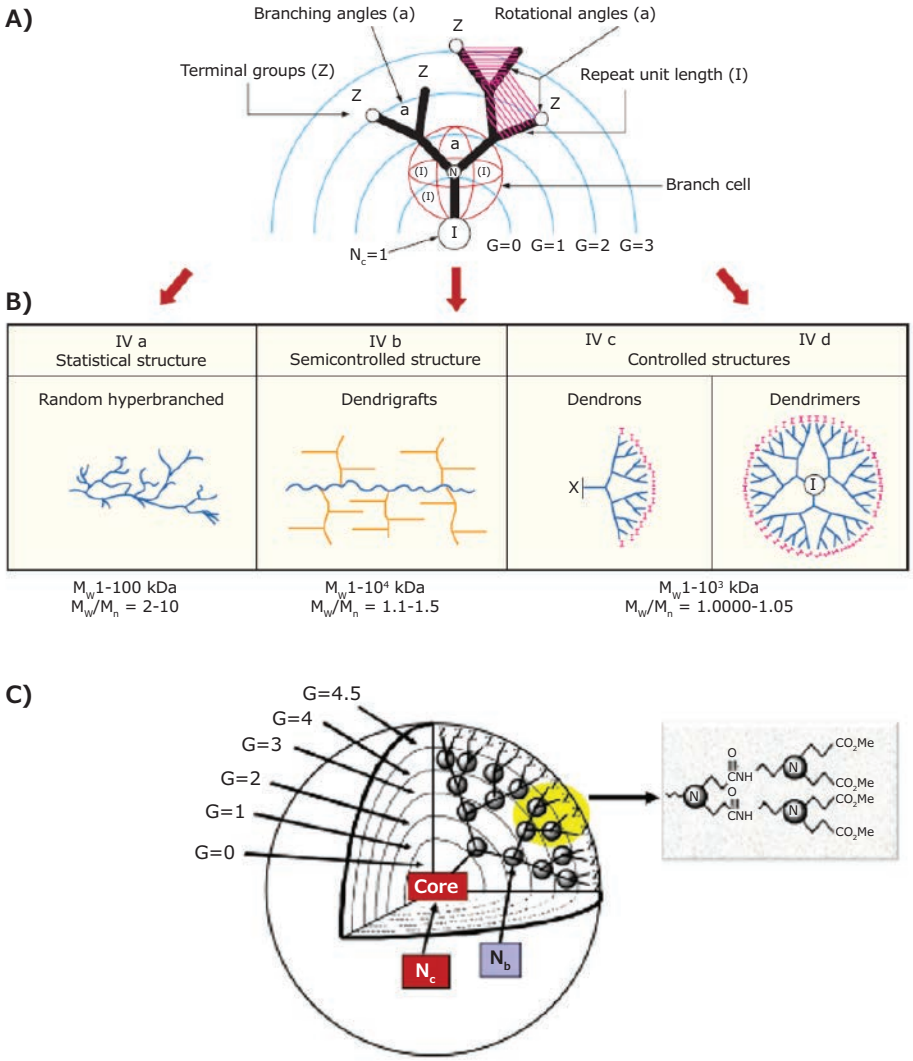

Number of Surface Groups: $Z=N_c N_b^G$

Number of Branch Cells: $BC=N_c N_b^{G-1}$

Molecular Weights: $MW=M_c + N_c [M_{RU} N_b^{G-1} + M_t N_b^G]$

Figure 1. A) Dendritic polymers are open, covalent assemblies of number of branches. B) Subclasses of Dendritic polymer (IVa-IVd). C) Mathematical expressions for calculating the theoretical number of surface groups (Z), branch cells (BCs), and molecular weights (M_ws) for PAMAM dendrimers as a function of generation for the PAMAM dendrimer family, where: N_c, N_b = core, branch cell multiplicities; respectively, and G = generation. Reprinted with permission from reference 3, copyright 2004 Sigma-Aldrich; reference 5, 2005 Elsevier; and reference 6, 2012 Cambridge University Press.

surface chemistry.[8,9] Systematically controlling/engineering these six CNDPs allows for developing "quantitative nanoscale structure versus activity" relationships (QNSAR). These unique dendrimer-based QNSAR relationships provide a simple and effective strategy for optimizing an almost unlimited number of desirable properties for a wide range of unmet needs and applications. More specifically, this dendrimer-based CNDP approach can potentially optimize supramolecular drug/guest encapsulation complexes or covalently conjugated active pharmaceutical drugs, usually via cleavable linkers, in concert with receptor functional targeting groups to the multifunctional dendrimer surface. These monodispersed, multifunctional dendrimer conjugates may be designed and engineered to specifically target designated receptor sites for various diseases, especially cancer.[9] These smart, disease-specific targeting features demonstrated by dendrimers are not readily available in other known traditional nanoparticle or polymeric platforms.[12] Many of these targeted, dendrimer-based conjugates (i.e., DEP®) are currently exhibiting unprecedented benefits in Phase II and III human clinical trials for the treatment of cancer (https://starpharma.com/drug_delivery).

Supramolecular or Covalent Chemical Attachment of Drugs for Delivery

A wide range of guest molecules (i.e., APIs) may be physically or chemically associated with dendrimers. The supramolecular approach generally involves interior encapsulation (i.e., unimolecular encapsulation) of guest molecules involving hydrogen bonding/Van derWaal forces within the interior void spaces of

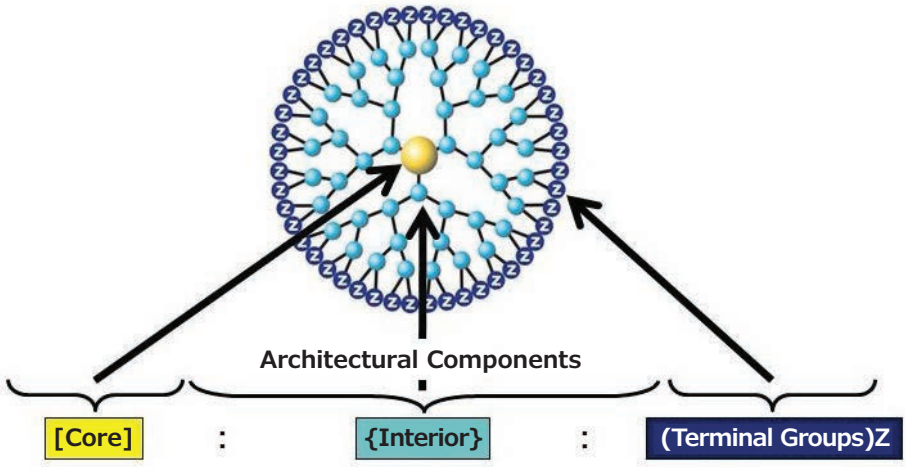

Figure 2. Architectural components of PAMAM dendrimer. Reprinted and modified with permission from NanoSynthons LLC.

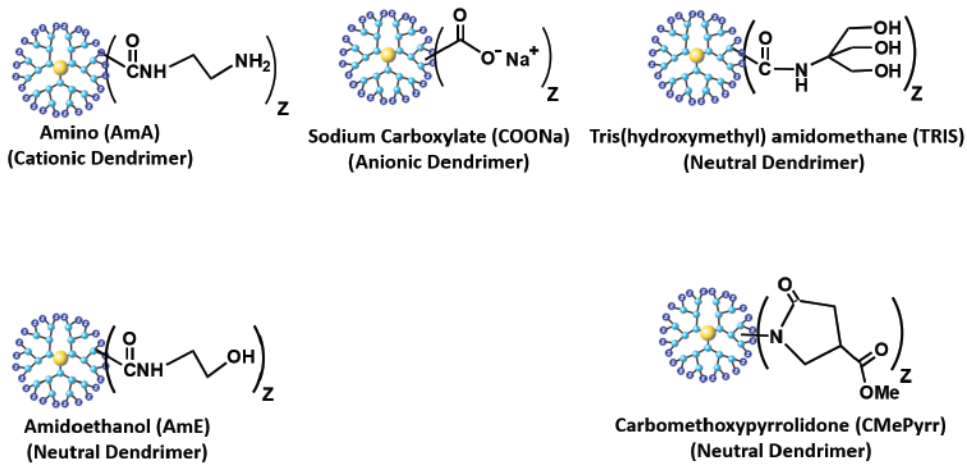

Figure 3. PAMAM Dendrimer compositions with various surface functionality. Reprinted and modified with permission from NanoSynthons LLC.

symmetrically branched dendrimers and /or by charge-charge interactions at the dendrimer surface. These supramolecular associations depend mainly upon the chemical features of the guest molecules, the amount of interior void space available (i.e., the dendrimer generation), and/or the surface chemistry features of the dendrimer.[10] The covalent chemical approach involves chemical conjugation of guest molecules with dendrimer surface moieties generally involving the integration of cleavable/ hydrolyzable amide, ester or disulfide bonds, etc. to provide a release mechanism for making the drug bioavailable after targeting to a specific disease site.[11]

Not All Dendrimers Exhibit Unimolecular Encapsulation Properties Based on Interior Void Space

Generally speaking, hundreds of dendrimer families have been synthesized and are available in an almost unlimited variety of elemental/functional compositions.[6] That withstanding, all known dendrimer compositions may be sub-divided into two major categories, namely; (1) those containing symmetrical branch cells (i.e., Tomalia, Vögtle, Fréchet, Newkome type dendrimers) and (2) those possessing asymmetrical branch cells (i.e., Denkewalter type dendrimers).[8] Essentially 99.5% of all reported dendrimer architectures possess symmetrical branch cell architecture (Category 1) in contrast to only a few examples of asymmetrical branch cell Denkewalter-type (Category 2) dendrimers. These asymmetrical dendrimers possess no available interior void space to allow unimolecular encapsulation of guest molecules.

Both dendrimer categories are recognized as offering many distinct advantages over conventional drug delivery systems. These advantages include: (a) precise, monodisperse nanoscale dimensions that may be (b) systematically enhanced as a function of generation, with (c) generationally dependent, mathematically defined numbers of surface groups that allow (d) the ability to attach desired multiples of drugs, targeting ligands or imaging agents, etc. by chemical conjugation. In the case of Category 1 dendrimers, multiple (hydrophobic and hydrophilic) drugs may be encapsulated within their interiors, usually, after dendrimer synthesis is completed, in contrast to micelles, liposomes, or other nanoparticles; wherein drugs are often encapsulated during

the synthesis.[12] As such, dendrimers are readily engineerable for use as advanced multifunctional systems with many unique features compared to conventional delivery systems. Most notable is the general use of highly water-soluble dendrimers as vehicles suitable for a wide range of administration modes, including intravenous, intranasal, ocular, oral, transdermal, and topical routes.[10,13]

Dendrimers for Drug Targeting to Specific Disease Sites

Dendrimers possess unique nanoscale dimensions and well-defined surface functionality that allow them to be more readily engineered for either (a) passive targeted or (b) receptor-mediated targeting compared to existing lipid or polymer-based drug delivery systems. Passive targeting (i.e., enhanced permeability and retention (EPR) effect), first pioneered by Maeda et al.,[14] is primarily defined by the ability of a drug carrier to deliver therapy through leaky tumor vasculatures surrounding the tumors and into cancer cells by passive diffusion. Important drug delivery vehicle parameters such as critical nanoscale dimensions and optimum multiples/types of vehicle surface functionality may be readily designed/engineered into dendrimer-based vectors.

Historically, the current strategy of "receptor-mediated, active targeting" was first demonstrated/ pioneered by Tomalia et al. as early as 1994. This targeted approach involved using G=3; PAMAM dendrimer conjugates bearing tumor-specific, monoclonal antibodies and chelated radioactive indium-111. This *in-vivo* study clearly demonstrated that tail fin injection of this targeting conjugate into athymic mouse models bearing human tumor xenografts produced tumor localization of this radiotherapy within 17 hrs with enhanced localization (i.e., 21.6 % of injected dose/gram of tissue) after 48 hrs. The successful use of these conjugated PAMAM dendrimers for active, receptor-mediated targeting therapy depends mainly on the ability to conjugate well-defined multiples of suitable targeting ligands (i.e., monoclonal antibodies, antibody fragments, or non-antibody ligands like peptide or small proteins) specific for binding overexpressed receptors residing at the target site. Dendrimers may be one of the most optimum platforms currently available for receptor-mediated targeting. This is primarily due to their monodispersity and mathematically defined conjugation sites.

A significant benefit expected from active targeting strategies using dendrimers is to enhance specific targeted cellular/ intracellular drug uptake while minimizing whole body exposure to any drug toxicity. Although using a single ligand targeting platform has improved targeting efficiency, receptor-mediated endocytosis has become saturated with therapy usage, ultimately limiting dendrimer-drug conjugate penetration during cellular uptake. To improve this situation, various research groups have attempted to develop a dual-ligand based targeted dendrimer system based on a multi-step conjugation process. However, this approach appears to have certain limitations due to "nanoscale sterically induced stoichiometry" effects (NSIS).[3,6,9,15] As such, an unmet need is to find an alternative to the multi-step chemical conjugation approach.

Heuristic Atom-Like Compounds at the Nanoscale Level; Dendrimers as Building Blocks to Create Stoichiometric Nano-compounds

Dendrimers are widely recognized as heuristic soft matter-nano elements much as fullerenes, viruses, DNA/RNA, or proteins, as proposed in a Nanomaterials Classification Roadmap. These proposed nano-elements were demonstrated to exhibit reactivities/ stoichiometric relationships at the nano level reminiscent of atomic level traditional elements found in the Mendeleev Periodic Table. In essence, it is possible to use dendrimers as reactive building blocks to design and synthesize more complex stoichiometric nano-compounds and nano-devices.

Unequivocal examples of dendrimers exhibiting elemental, atom-like properties have demonstrated the synthesis of prior predicted stoichiometric nano-compounds. These stoichiometric nano-compounds are referred to as "surface saturated core-shell (tecto) dendrimers.[16] The maximum number of "shell dendrimers" that may occupy the surface space surrounding a specific "core dendrimer" is defined by the ratio of the respective core/shell dendrimer radii (i.e., r_1/r_2) and the Mansfield-Tomalia-Rakesh equation. As such, the maximum number of spheroidal "shell dendrimers" that may be associated with a specific spheroidal "core dendrimer" may be predicted by the generational dimensions of the core and shell dendrimers, respectively as described in **Figure 4**. In all cases, these predictions were very accurately fulfilled by the actual synthesis and characterization of these stoichiometric nanoscale compounds. In general, these multi-dendrimer or core-shell structures are referred to as megamers.[3,17]

Further corroboration of these nanoscale principles and rules was demonstrated by the covalent attachment of spheroidal fullerenes to form a shell surrounding the surface of a designated spheroidal core dendrimer. Characterization of this dendrimer (core)–fullerene (shell) nano-compound revealed an experimental stoichiometry of 30:1 versus a predicted value of 32:1, based on the ratio of core dendrimer: shell fullerene radii, respectively.[18,19]

Dendrimer-Based CNDP Engineering for New Properties

Our group has continued to explore specific dendrimer structures, as well as their covalent nano-compounds and supramolecular nano-assemblies as a function of core, branch cell symmetry, interior elemental composition, shape, size (i.e., generations), and surface chemistry. These studies focus on a deeper understanding of how these CNDPs influence known properties, as well as the potential creation of new unpredicted properties of interest to nanomedicine or the development of new advanced materials. A recent example is the unexpected discovery of "dendrimer dipole" induced generation of terahertz radiation which occurred based on the systematic engineering of certain CNDPs associated with Tomalia-type PAMAM dendrimers.[20,21] These dendrimer-based terahertz generators are the critical component required for new commercially available terahertz spectrometers produced by Applied Research & Photonics.

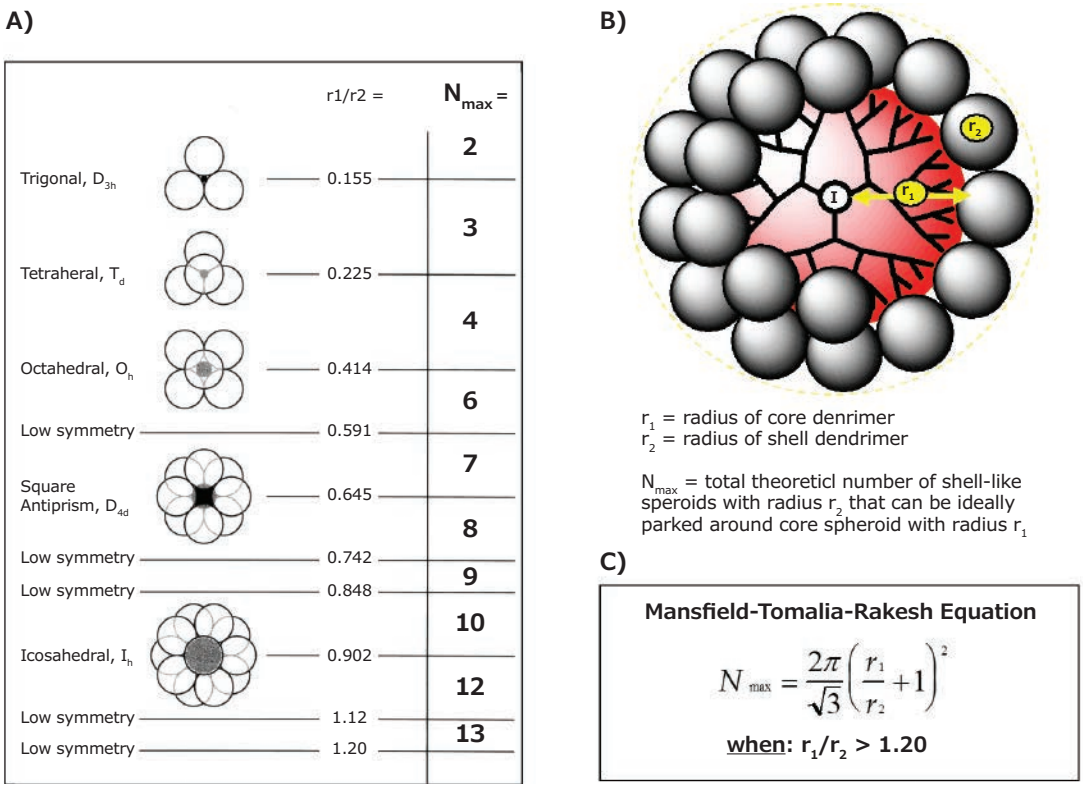

Figure 4. A) Symmetry properties of core-shell structures, where $r_1/r_2 < 1.2$. B) Sterically induced stoichiometry based on the respective radii of core and shell dendrimers. C) Mansfield-Tomalia-Rakesh equation for calculating maximum shell filling when $r_1/r_2 > 1.2$. Reprinted with permission from reference 3, copyright 2004 Sigma-Aldrich.

Similarly, particular surface-engineered PAMAM dendrimers (i.e., pyrrolidone terminated) have been found to exhibit stealth-like properties similar to Pegylated drugs (U.S. Patent 10,968,176B2, Tomalia, Hedstrand and Nixon, 2021). Whereas other surface modified PAMAM dendrimers,[22] as well as specific Janus type dendron structures, are active as delivery vehicles for mRNA in the production of effective RNA vaccines against COVID-19 viruses and other pathogens.[23]

Dendrimer-Dendrimer Nano-Assemblies (Hybrid Dendrimers)

Similar CNDP engineering involving two or more different dendrimers has shown that they may be combined to work in a unique tandem type system to achieve new therapeutically desired release profiles. More specifically, it was found that PAMAM dendrimers may be simply combined (i.e., no covalent chemical reaction) to create new hybrid dendrimer compositions. (PCT/US2007/014402, Chauhan and Svenson, 2007). These hybrid dendrimers displayed an intermediate drug profile that may be predicted based on individual dendrimer behavior.[12,24,25]

This "hybrid dendrimer concept" involves combining two or more CNDP differentiated dendrimers possessing appropriate surface groups to form "non-covalent, multi-dendrimer" compositions. This generally involves combining carboxylic acid and amine surface moieties, wherein charge neutralized salts are formed at the connection interface. The objective is to capture certain unique features associated with the individual participating dendrimers by hybridizing these CNDP differentiated dendrimers to produce a multi-dendrimer nano-assembly without any covalent chemical reactions (**Figure 5**). This "hybrid dendrimer concept" may be visualized as a simple strategy for bypassing more complex covalent chemistry steps to prepare sophisticated dendrimer nanodevices exhibiting multiple ligands, imaging moieties, or drug molecules. In brief, the hybrid dendrimer concept may be viewed as a 'click'-type CNDP engineering protocol for engineering certain desired features within a specific dendritic platform. These non-covalent, click-chemistry-based hybrid dendrimers provide a facile and rapid method for creating more complex, multifunctional dendritic platforms versus current multi-step covalent conjugation chemistry protocols.

An unprecedented feature of such a "hybrid dendrimer system" was demonstrated by observing a completely unexpected efficacy for oral delivery of docetaxel (DTX) versus traditional intravenous drug injection. Very briefly, simple oral administration of DTX in a hybrid dendrimer formulation exhibited a remarkable pharmacokinetic (PK) profile which was shown to be completely equivalent to a more invasive, complicated intravenous injection of commercially available docetaxel (Taxotere®). The PK parameters associated with the hybrid dendrimer formulations revealed a substantially higher potential for supporting the DTX plasma circulation time. Furthermore, the DTX-loaded hybrid dendrimer formulations exhibited higher area under the curve (AUC) and area under the moment curve (AUMC) than DTX loaded in either cationic (i.e., amine terminated) or anionic (i.e., carboxylate terminated) dendrimers, respectively. Moreover, the AUC of commercially available Taxotere® (intravenous) was almost parallel to orally

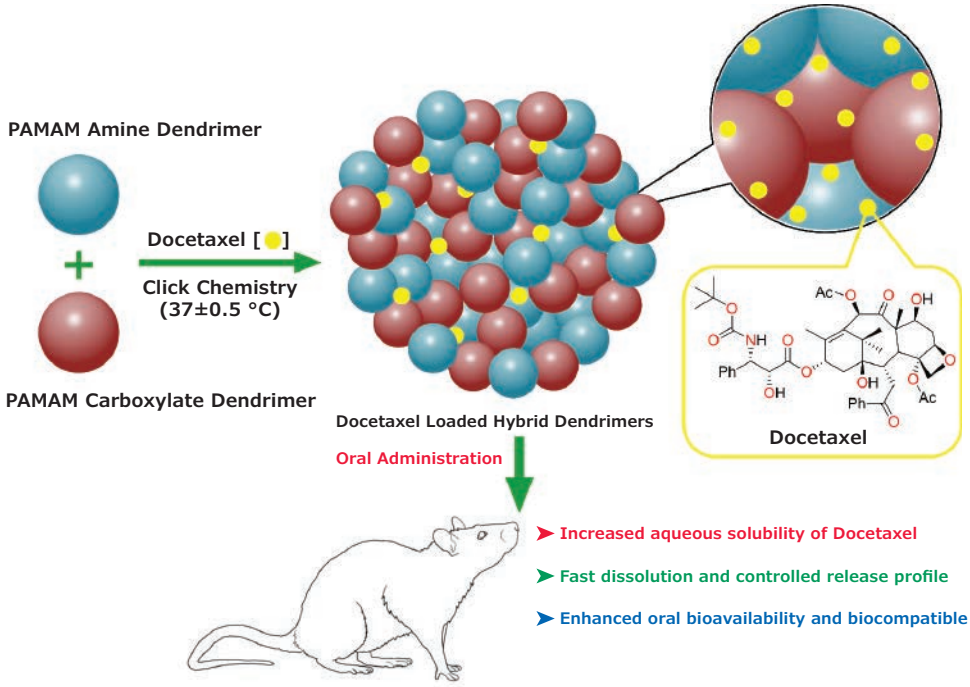

Figure 5. Schematic diagram showing strategy for developing hybrid dendrimer-based nano-assembly of docetaxel and its role in enhancing aqueous solubility, modifying the dissolution and release profile with superior oral bioavailability. Reprinted and modified with permission from reference 12, copyright 2019 Elsevier.

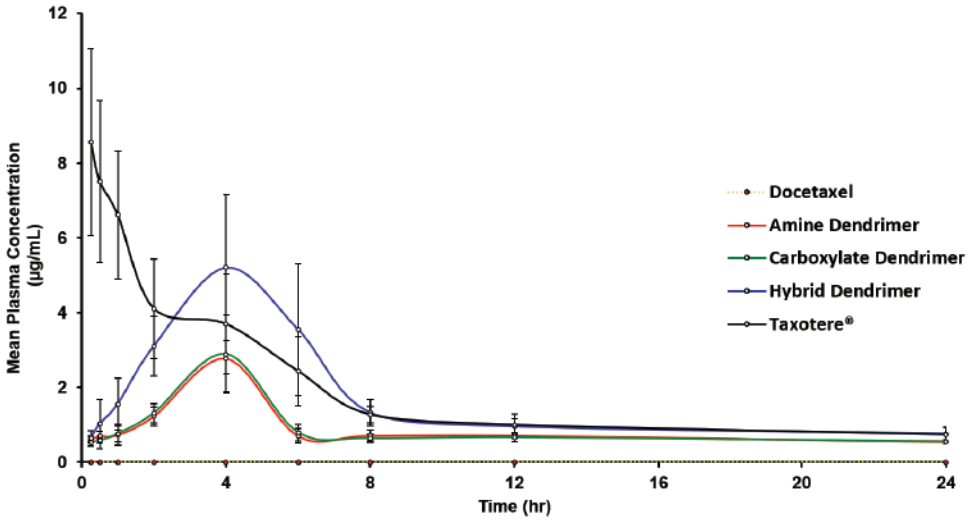

Figure 6. Comparative mean plasma concentration-time profile of docetaxel with various dendrimers (Amine, Carboxylate, and Hybrid) (Mean±SD; n=8) and intravenous marketed formulation of DTX (Taxotere®) (Mean±SD; n=4) at a dose of 10mg/kg body weight in SD rat. Reprinted and modified with permission from reference 12, copyright 2019 Elsevier.

administered hybrid dendrimer formulations and higher than either individual anionic or cationic terminated dendrimers (Figure 6).

Dendrimer-Nanoparticle (i.e., albumin) Hybrid Nano-Assemblies

Although few examples of dendrimer-soft nanoparticle hybrids have been reported, cationic G4 PAMAM dendrimers have been tethered by the self-assembly with anionic albumin (Tekade et al. 2015). These unique dendrimer-albumin hybrid systems were utilized to entrap paclitaxel within the dendrimer components; whereas the albumin components of the hybrid system were used to anchor specific targeting ligands. These dendrimer-albumin hybrid nano-assemblies exhibited enhanced inhibition of cancer cells compared to paclitaxel in combination with albumin nanoparticles.[25]

Conclusion

After nearly four decades since the discovery of dendrimers, the quantized nature and mathematically defined components of these structures are becoming more fully recognized. Six well-defined "critical nanoscale design parameters" (CNDPs) of dendrimers: architecture, elemental composition, flexibility/rigidity, shape, size, and surface chemistry are now being

systematically engineered to provide optimized candidates for many commercial applications. These diverse applications range from their use as terahertz generators to targeting vectors for drug delivery. Recent work has shown that supramolecular, non-covalently bonded assemblies of dendrimers referred to as "hybridized dendrimer nano-assemblies" appear to capture unique CNDP features manifested by their individual dendrimer components, producing novel high value properties in the delivery of drugs. The multi-dendrimer nanoelements can be welded together to create sophisticated nano-compounds with the ability to communicate, stay in sync, and develop biological machines for advanced therapeutic applications.

Acknowledgment

We are grateful to Ms. Linda S. Nixon, NanoSynthons LLC (MI, USA), for the critical graphics and editing of this manuscript.

References

(1) Tomalia, D. A.; Baker, H.; Dewald, J.; Hall, M.; Kallos, G.; Martin, S.; Roeck, J.; Ryder, J; Smith, P. *Polym. J.* **1985**, *17* (1), 117–132.
(2) Tomalia, D. A.; Fréchet, J. M. *J. Polym. Sci., Part A: Polym. Chem.* **2002**, *40* (16), 2719–2728.
(3) Tomalia, D. A. *Aldrichimica Acta* **2004**, *37* (2), 39–57.
(4) Tomalia, D. A. *Prog. Polym. Sci.* **2005**, *30* (3–4), 294–324.
(5) Tomalia, D. A. *Mater. Today* **2005**, *8* (3), 34–46.
(6) Tomalia, D. A.; Christensen, J. B.; Boas, U. Cambridge University Press **2012**.
(7) Chauhan, A.; Krynicka, D.; Singh, M. K. Pharmaceutical Applications of Dendrimers, Elsevier **2020**.
(8) Tomalia, D. A.; Nixon, L. S.; Hedstrand, D. M. *Biomolecules* **2020**, *10* (4), 642.
(9) Chauhan, A. S.; Kaul, M. *J. Nanoparticle Res.* **2018**, *20* (9), 1–11.
(10) Chauhan, A.; Anton, B.; Singh, M. K. Pharmaceutical Applications of Dendrimers, Elsevier **2020**.
(11) Pentek, T.; Newenhouse, E.; O'Brien, B.; Chauhan, A. S. *Molecules* **2017**, *22* (1), 137.
(12) Singh, M. K.; Kuncha, M.; Nayak, V. L.; Sarma, A. V.; Kumar, M. J. M.; Chauhan, A. S.; Sistla, R. *Nanomed.: Nanotechnol. Biol. Med.* **2019**, *21*, 102043.
(13) Svenson, S.; Chauhan, A. S. *Future Med.* **2008**, *3*, 679–702.
(14) Maeda, H. *J. Pers. Med.* **2021**, *11* (3), 229.
(15) Tomalia, D. A.; Klajnert-Maculewicz, B.; Johnson, K. A. M.; Brinkman, H. F.; Janaszewska, A.; Hedstrand, D. M. *Prog. Polym. Sci.* **2019**, *90*, 35–117.
(16) Uppuluri, S.; Swanson, D. R.; Piehler, L. T.; Li, J.; Hagnauer, G. L.; Tomalia, D. A. *Adv. Mater.* **2000**, *12* (11), 796–800.
(17) Li, J.; Swanson, D. R.; Qin, D.; Brothers, H. M.; Piehler, L. T.; Tomalia, D.; Meier, D. J. *Langmuir* **1999**, *15* (21), 7347–7350.
(18) Kujawski, M.; Rakesh, L.; Gala, K.; Jensen, A.; Fahlman, B.; Feng, Z.; Mohanty, D. K. *J. Nanosci. Nanotechnol.* **2007**, *7* (4–5), 1670–1674.
(19) Jensen, A. W.; Maru, B. S.; Zhang, X.; Mohanty, D. K.; Fahlman, B. D.; Swanson, D. R.; Tomalia, D. A. *Nano Lett.* **2005**, *5* (6), 1171–1173.
(20) Rahman, A.; Rahman, A. K.; Rao, B. *Biosens.* **2016**, *82*, 64–70.
(21) Rahman, A.; Rahman, A. K.; Tomalia, D. A. *Nanoscale Horiz.* **2017**, *2* (3), 127–134.
(22) Chahal, J. S.; Khan, O. F.; Cooper, C. L.; Mc Partlan, J. S.; Tsosie, J. K.; Tilley, L. D.; Sidik, S.M.; Lourido, S.; Langer, R.; Bavari, S.; Ploegh, H.L.; Anderson, D. G. *Proc. Natl. Acad. Sci.* **2016**, *113* (29), E4133–E4142.
(23) Zhang, D.; Atochina-Vasserman, E. N.; Maurya, D. S.; Huang, N.; Xiao, Q.; Ona, N.; Liu, M.; Shahnawaz, H.; Ni, H.; Kim, K.; Billingsley, M.M.; Pochan, D. J.; Mitchell, M. J.; Weissman, D.; Percec, V. *J. Am. Chem. Soc.* **2021**, *143* (31), 12315–12327.
(24) Singh, M. K.; Pooja, D.; Kulhari, H.; Jain, S. K.; Sistla, R.; Chauhan, A. S. *Eur. J. Pharm. Sci.* **2017**, *96*, 84–92.
(25) Tekade, R. K.; Tekade, M.; Kumar, M.; Chauhan, A. S. *Pharm. Res.* **2015**, *32* (3), 910–928.

Dendrimers

Polyester bis-MPA Dendrimers

Name	Generation	Surface	No. Of Surface Groups	Cat. No.
Bis-MPA-NHBoc dendrimer	4	Boc-protected amine	48	**901322-100MG**
	4	NHBoc, alkyne (core)	16	**901313-100MG**
	2	NHBoc, alkyne (core)	4	**901316-100MG**
	4	NHBoc, azide (core)	16	**901298-100MG**
	2	NHBoc, azide (core)	4	**901297-100MG**
	1	NHBoc, azide (core)	2	**901311-100MG**
	4	NHBoc, thiol (core)	16	**901304-100MG**
	3	NHBoc, thiol (core)	8	**901303-100MG**
	2	NHBoc, thiol (core)	4	**901312-100MG**
	1	NHBoc, thiol (core)	2	**901300-100MG**
	3	trimethylol propane core	24	**901329-100MG**
	2	trimethylol propane core	12	**901330-100MG**
	1	trimethylol propane core	6	**901333-100MG**
Bis-MPA-RAFT dendrimer	1	trimethylol propane core	6	**911550-250MG**
Poly(ethylene glycol) linear dendrimer	5	carboxyl terminated	64	**911186-500MG**
	4	carboxyl terminated	32	**911364-500MG**
	3	carboxyl terminated	16	**911259-500MG**
Poly(ethylene glycol) linear dendron	4	carboxyl terminated	16	**911240-250MG**
	2	carboxyl terminated	4	**911321-250MG**
	1	carboxyl terminated	2	**911313-250MG**

Name	Generation	Surface	No. Of Surface Groups	Cat. No.
Polyester bis-MPA dendron	3	acetylene, NHBoc (core)	8	**901376-100MG**
	2	acetylene, NHBoc (core)	4	**901374-100MG**
	1	acetylene, NHBoc (core)	2	**901370-100MG**
	2	azide, NHBoc (core)	4	**901335-100MG**
	2	carboxyl, biotin (core)	4	**911348-50MG**
	1	carboxyl, biotin (core)	2	**911275-50MG**
	4	carboxyl, NHBoc (core)	16	**901381-100MG**
	4	carboxyl, NHBoc (core)	16	**901394-100MG**
	3	carboxyl, NHBoc (core)	8	**901380-100MG**
	3	carboxyl, NHBoc (core)	8	**901398-100MG**
	2	carboxyl, NHBoc (core)	4	**901408-100MG**
	1	carboxyl, NHBoc (core)	2	**901379-100MG**
	2	carboxyl, Rhodamine (core)	4	**911496-50MG**
	3	NHBoc, biotin (core)	8	**911437-50MG**
	2	NHBoc, biotin (core)	4	**911569-50MG**
	1	NHBoc, biotin (core)	2	**911577-50MG**
	2	NHBoc, carboxyl (core)	4	**901377-100MG**
	3	NHBoc, NHS (core)	8	**911518-50MG**
	2	NHBoc, NHS (core)	4	**911488-50MG**
	1	NHBoc, NHS (core)	2	**911461-50MG**
	2	rhodamine, carboxyl (core)	4	**911445-50MG**
	3	carboxyl, biotin (core)	8	**911291-50MG**
	1	carboxyl, NHBoc (core)	2	**901393-100MG**
	3	NHBoc, azide (core)	8	**901332-100MG**

PAMAM Dendrimers

Name	Generation	Surface	No. Of Surface Groups	Cat. No.
PAMAM dendrimer, 10 wt. % in methanol	6	1,4-diaminobutane core	256	**596426-2G**
	5	cystamine core	128	**648159-1G**
	4	ethylenediamine core	64	**412449-2.5G** **412449-10G**
	3.5	ethylenediamine core	64	**412430-2.5G** **412430-10G**
	2.5	ethylenediamine core	32	**412414-2.5G** **412414-10G**
PAMAM dendrimer, 20 wt. % in methanol	1	1,4-diaminobutane core	8	**595861-2G**
	2	cystamine core	16	**647829-1G**
	3	ethylenediamine core	32	**412422-5G** **412422-25G**
	2	ethylenediamine core	16	**412406-25G** **412406-5G**
	1.5	ethylenediamine core	16	**412392-1G** **412392-5G**
	1	ethylenediamine core	8	**412384-5G** **412384-25G**
	0.5	ethylenediamine core	8	**412376-5G**
	0.0	ethylenediamine core	4	**412368-5G** **412368-25G**
PAMAM dendrimer, 5 wt. % in methanol	10	ethylenediamine core	4096	**536776-2G**
	9	ethylenediamine core	2048	**536768-2G**
	8	ethylenediamine core	1024	**536741-2.5G**
	7	ethylenediamine core	512	**536725-2.5G**
	6.5	ethylenediamine core	512	**536792-2.5G**
	6	ethylenediamine core	256	**536717-5G**
	5.5	ethylenediamine core	256	**536784-5G**
	5	ethylenediamine core	128	**536709-5G**
	4.5	ethylenediamine core	128	**470457-2.5G** **470457-10G**

Name	Generation	Surface	No. Of Surface Groups	Cat. No.
PAMAM dendrimer, powder	0	ethylenediamine core	4	**526142-1G**
PAMAM-25% C12 dendrimer, 10 wt. % in methanol	4	ethylenediamine core	64	**536962-5G**
	3	ethylenediamine core	32	**536865-10G**
	2	ethylenediamine core	16	**536849-10G**
PAMAM-50% C12 dendrimer, 10 wt. % in methanol	4	ethylenediamine core	64	**536970-5G**
PAMAM-OH dendrimer, 10 wt. % in methanol	4	ethylenediamine core	64	**477850-2.5G** **477850-10G**
PAMAM-OH dendrimer, 20 wt. % in methanol	3	ethylenediamine core	32	**477842-5ML**
	2	ethylenediamine core	16	**477834-5ML** **477834-25ML**
PAMAM-OH dendrimer, 5 wt. % in methanol	7	ethylenediamine core	512	**536830-2.5G**
	6	ethylenediamine core	256	**536822-5G**
	5	ethylenediamine core	128	**536814-5G**
PAMAM-succinamic acid dendrimer, 10 wt. % in H_2O	5	1,4-diaminobutane core	128	**635898-1G**
	4	1,4-diaminobutane core	64	**635871-1G**
PAMAM Dendrimer Kit	4-7	ethylenediamine core	64-512	**664049-1KT**
	0-3	ethylenediamine core	4-32	**664138-1KT**

PEG Dendrimers

Name	Generation	Surface	No. Of Surface Groups	Cat. No.
Hyperbranched PEG 6k	6	hydroxyl, PEG 6,000 (core)	128	**806234-5G**
	5	hydroxyl, PEG 6,000 (core)	64	**806226-5G**
	4	hydroxyl, PEG 6,000 (core)	32	**806218-5G**
Hyperbranched PEG 10k	6	hydroxyl, PEG 10,000 (core)	128	**806285-5G**
	5	hydroxyl, PEG 10,000 (core)	64	**806277-5G**
	4	hydroxyl, PEG 10,000 (core)	32	**806269-5G**
	3	hydroxyl, PEG 10,000 (core)	16	**806250-5G**
	2	hydroxyl, PEG 10,000 (core)	8	**806242-5G**
Hyperbranched PEG 20k	6	hydroxyl, PEG 20,000 (core)	128	**806331-5G**
	5	hydroxyl, PEG 20,000 (core)	64	**806315-5G**
	4	hydroxyl, PEG 20,000 (core)	32	**806323-5G**
	3	hydroxyl, PEG 20,000 (core)	16	**806307-5G**
	2	hydroxyl, PEG 20,000 (core)	8	**806293-5G**
Poly(ethylene glycol) linear dendrimer	5	carboxyl terminated, PEG 10,000 (core)	64	**911186-500MG**
	4	carboxyl terminated, PEG 10,000 (core)	32	**911364-500MG**
	4	NHBoc terminated, PEG 6,000 (core)	32	**901397-250MG**
	3	NHBoc terminated, PEG 6,000 (core)	16	**901407-250MG**
	2	NHBoc terminated, PEG 6,000 (core)	8	**901382-250MG**

MERCK

EVERYTHING BUT THE KITCHEN SINK

Comprehensive biodegradable polymers for drug delivery

Biodegradable polymers contain polymer chains that are hydrolytically or enzymatically cleavable, resulting in biocompatible or nontoxic by-products. They are widely used in drug delivery research to achieve controlled and targeted delivery of therapeutic agents (e.g. APIs, genetic material, peptides, vaccines, and antibiotics).

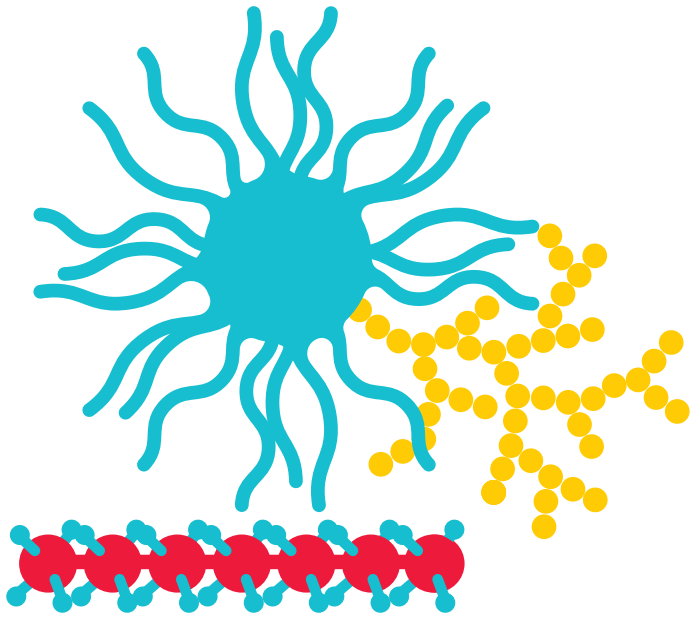

We now offer the following classes of high-purity biodegradable polymers:

- Poly (lactide-co-glycolide) copolymers (PLGA)
- Poly(lactic acid) (PLA)
- Poly(caprolactone) (PCL)
- Amphiphilic block copolymers
- End-functionalized biodegradable polymers

For more information, please visit:
SigmaAldrich.com/resomer

Polymeric Antioxidants and Nanobiomaterials for Innovative Therapeutic Modalities

Ilker S. Bayer

Smart Materials, Istituto Italiano di Tecnologia,
Via Morego 30 Genova, 16163, Italy.
E-mail: ilker.bayer@iit.it

Introduction

Oxidative stress is a critical element of associating environmental toxicity with the multistage carcinogenic process. Reactive oxygen species (ROS) or reactive oxygen and nitrogen species (RONS) are generated in response to both endogenous (from within) and exogenous (outside) stimuli. To counterbalance RONS-mediated damage, an endogenous antioxidant defense system is activated. However, when the degree of oxidation exceeds such preventive mechanisms, oxidative stress arises. Chronic and cumulative oxidative stress induces various modifications to essential biological macromolecules such as DNA, lipids, and proteins. It is also a key source of side effects associated with standard cancer treatments. Antioxidant supplementation, including vitamins A, C, and E, and polyphenols, such as tannic acid, gallic acid, and epigallocatechin gallate (EGCG), can reduce adverse reactions and toxicities related to oxidative stress and have been proven effective through various clinical studies. Despite their strong potential, very few antioxidants are approved in medicine due to several limitations such as low stability, poor water solubility, low bioavailability, and short circulation time in the bloodstream leading to low antioxidant efficiency and longevity.[1,2,3]

To circumvent limitations associated with antioxidant supplements, antioxidant polymers are considered effective new generation antioxidant therapies.[4,6]. Polymeric antioxidants have prolonged stability and circulation and can avoid rapid clearance by the immune system, resulting in better bioavailability and antioxidant potential. Furthermore, since polymers can be engineered into several useful forms such as films, gels, solutions, and nanoparticles, antioxidant polymers can be delivered to the site of interest and release encapsulated drugs in a controlled response to inflammatory environments. Antioxidant polymer platforms can be designed to respond to several biological factors such as pH, redox potential, and enzymes, as well as exogenous stimuli such as light, magnetism, ultrasound, and X-rays (**Figure 1**). As such, antioxidant polymeric platforms serve as transport vehicles for effective drug delivery and seamlessly act as RONS scavengers throughout the therapeutic process.

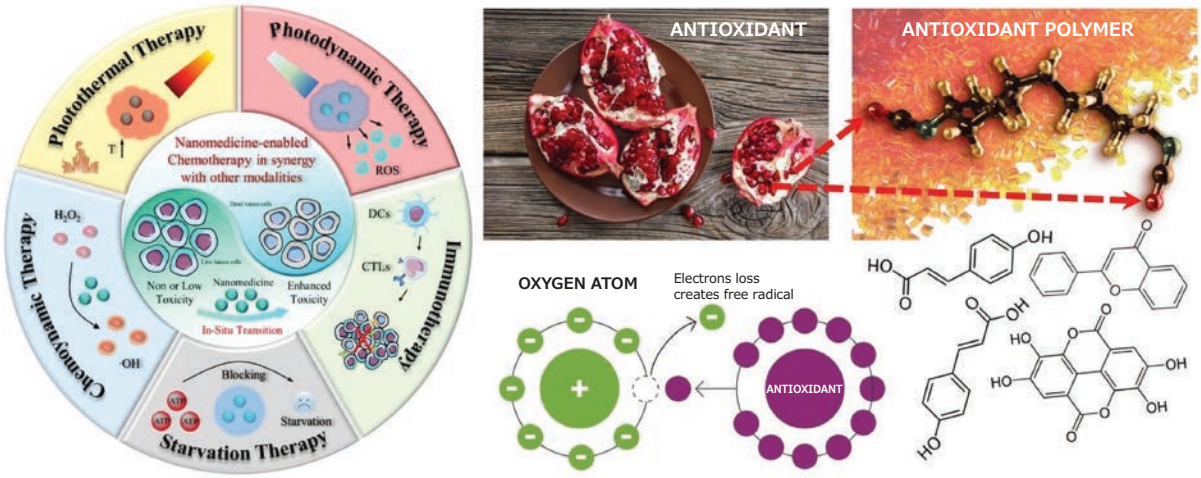

Figure 1. A) A schematic representation of several nanomedicine-enabled chemotherapy routes and related cancer therapies. Reprinted with permission from reference 9, copyright 2022 Springer. **B**) Antioxidant molecules can be extracted from several different plants, fruits, and even their waste after being processed. They can effectively reduce or eliminate electron-loss related free radical formation in metabolic systems. Reprinted with permission from reference 4, copyright 2021 Multidisciplinary Digital Publishing Institute.

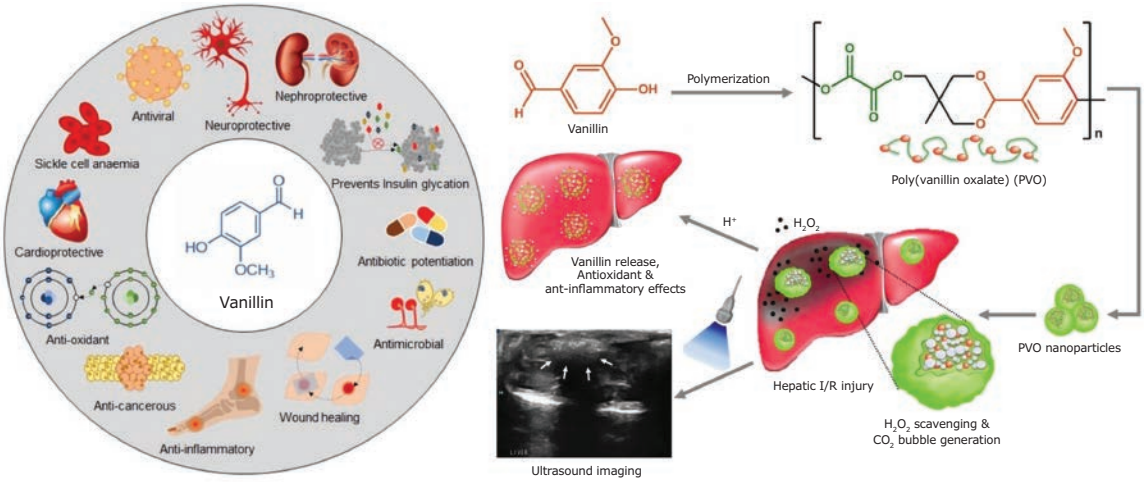

Figure 2. A) The antioxidant molecule, vanillin. This natural extract can easily be polymerized, but as a molecule, it has been shown to display excellent therapeutic properties such as anticancer, antioxidant, anti-inflammatory, neuroprotective, anti-sickling, anti-amyloid aggregation, and inhibition of non-enzymatic glycation, antibacterial, anti-fungal, anti-quorum sensing, antibiotic potentiation, wound healing/tissue engineering, and antiviral. Reprinted with permission from reference 15, copyright 2021 Springer Singapore. B) A schematic diagram illustrating antioxidant PVO polymer with H_2O_2-triggered echogenic properties and intrinsic antioxidant and anti-inflammatory activities. Treatment with PVO increases the echo intensity for ultrasound imaging and exerts therapeutic effects in H_2O_2-accompanying ischemia/reperfusion (I/R) injury. Reprinted with permission from reference 14, copyright 2016 Elsevier.

Polymers With Antioxidant Moieties

Historically, polymers with antioxidant moieties were first developed industrially to prevent polymers from oxidative degradation. For instance, polypropylene was rendered resistant against oxidative degradation by attaching cross-linkable antioxidant moieties to the main chain.[7] Biotechnology and biomedicine applications have modified biomedical polymers similarly to scavenge ROS and RONS, such as grafting ellagic acid to chitosan.[8] Likewise, vanillin, a powerful natural antioxidant (**Figure 2A**), can crosslink with chitosan and, as such, it increases its mechanical properties and transforms chitosan into an antioxidant polymer.[10]

In addition, new antioxidant polymers are being synthesized via chemo-enzymatic methods such as biobased linear aliphatic-aromatic oligomers from ferulic acid and *trametes versicolor laccase*.[11] High molecular weight hydroxycinnamate-derived polymers from *Symphytum asperum Lepech* (a flowering plant) were also demonstrated to be effective antilipoperoxidants (depletes lipid oxidation). This is important because oxidative stress and lipid peroxidation levels can increase during different therapeutic modalities in cancer treatment, contradicting the treatment itself.[12,13]

In medical sciences, liver-related hepatic ischemia/reperfusion (I/R) injury is strongly associated with H_2O_2-mediated oxidative stress and is a crucial arbiter of cellular and tissue damage. Therefore, H_2O_2 is a significant therapeutic target for oxidative stress-associated inflammation. Poly(vanillin oxalate) (PVO) polymer (**Figure 2B**) generates CO_2 through H_2O_2-triggered oxidation of peroxalate esters and releases vanillin, which exerts antioxidant and anti-inflammatory activities and inhibits inflammation and apoptosis.[14] Recently, synthesizing antioxidant polymers from lignin derivatives is also of significant interest.[4] Phenols with various chemical structures can be obtained from lignin deconstruction; among them, vanillin and ferulic acid. Various polymers can be synthesized via different chemical modifications and polymerization pathways.

Unlike vehicle-based antioxidant depot approaches, covalently tethering antioxidants to polymers can enable a higher relative antioxidant content by increasing its longevity and presence. The structural incorporation of antioxidant moieties into polymers may offer more flexibility in applying polymer systems for therapeutic use, whereas encapsulation approaches are often limited to particle systems. Among common antioxidant supplements, vitamins A, C, and E are especially interesting for polymerization. These three vitamins are well known as antioxidants, and their low to no toxicity and regulatory approval make them advantageous to alternative new materials. However, many vitamins have very low tolerance for light, heat, and moisture exposure, complicating bioactivity retention during polymerization or grafting.[16] Even though their copolymerization is not necessarily straightforward, grafting vitamins to biomedical polymers while retaining a strong antioxidant effect can provide identical antioxidant protection *in vivo* to the vitamin alone.

Retinoic acid, the most biologically active form of vitamin A, plays an essential role in the induction of cell differentiation and the arrest of cell proliferation. It has been used in stem cell engineering and cancer therapy, particularly in differentiation therapy for acute myelogenous leukemia. However, it has deficient blood circulation levels due to rapid metabolization by the liver. The circulation can be improved by grafting retinoic acid to water-soluble chitosan oligosaccharide to form an antioxidant polymer drug.[17] Similarly, an interesting study on vitamin E showed that Trolox, a synthetic antioxidant and water-soluble analog of vitamin E, was polymerized to form an oxidation active polymer as a new class of biomaterial. This antioxidant polymer inhibited intracellular ROS formation and reduced basal ROS levels in monocytes and endothelial cells. It also effectively inhibited direct effects of oxidative stress like protein carbonyl formation, 3-nitrotyrosine levels, and 4-hydroxy-2-trans-nonenal levels in endothelial cells.[18]

Metal-chelating Intrinsically Antioxidant Polymers

Chelating drugs and chelator metal complexes are needed to prevent, diagnose, and treat cancer. Both cancer and normal cells require essential metal ions such as iron, copper, and zinc for growth and proliferation. Chelators can target the metabolic pathways of cancer cells by controlling proteins involved in regulating these metals. However, excess metal ion uptake by the cells can trigger and catalyze RONs, and special chelators can potentially inhibit the oxidative free radical damage on DNA caused by iron and copper catalytic centers. Specifically, chelating excess iron in the body can effectively fight tumors and side effects of certain cancer therapeutic modalities. To this end, a newly synthesized poly(1,8-octanediol-*co*-citrate-*co*-ascorbate) (POCA), a citric-acid based biodegradable elastomer with native and intrinsic antioxidant properties, could be a promising start (**Figure 3A**). POCA, synthesized from 1,8-octanediol, citric acid, and ascorbic acid, reduced ROS generation in cells and protected cells from oxidative stress-induced cell death (**Figure 3B**). Importantly, POCA antioxidant properties remained present upon degradation.[19]

Another very effective antioxidant polymer with metal chelating capability was demonstrated as a biodegradable, thermoresponsive gel with intrinsic antioxidant properties suitable for the delivery of therapeutics. Citric acid, poly(ethylene glycol) (PEG), and poly-*N*-isopropylacrylamide (PNIPAAm) were copolymerized by sequential polycondensation and radical polymerization to produce poly(polyethylene glycol citrate-*co*-*N*-isopropylacrylamide) (PPCN).[20] PPCN exhibited free radical scavenging activity, chelated iron ions, and inhibited lipid peroxidation while enabling chemokine delivery in a controlled manner (**Figure 4A**). Additionally, PPCN immediately formed a macroscopic gel in situ when injected into rat subcutaneous tissue, facilitated new connective tissue formation with a minimal foreign body response, and was resorbed by the body at 30 days post-implantation (**Figures 4B–D**).

Desferrioxamine (DFO), deferiprone (DFP), desferasirox (DFX), and ethylenediaminetetraacetic acid (EDTA) are currently the only FDA-approved metal-chelating compounds for specific removal of metals from the metabolism. Despite FDA approval, these compounds have limited bioavailability, insufficient selectivity, neurotoxicity, and other conflicting results on therapeutic performance, particularly regarding EDTA. A new DFO polymer system was developed by glycidol ring opening and aldehyde reactions with sodium periodate. The polymeric iron chelator was synthesized by conjugating DFO into hyperbranched polyglycerol (HPG) and resulted in improved circulation lifetimes and removal of excess iron *in vivo*. Additionally, the polymer effectively regulated plasma ferritin levels, which could potentially benefit patients suffering from transfusion iron overload.[21] A range of iron binding dendrimers terminated with hexadentate ligands derived from hydroxypyridinone, hydroxypyranone, and catechol moieties were synthesized to serve as clinically useful iron (III)-selective chelator polymers. The iron chelating abilities of these and similar polymers should be considered, for instance, for potential iron overload after tandem high-dose chemotherapy and autologous stem cell transplantation in patients with high-risk neuroblastoma.[22]

One unique application of metal-chelating polymers is in highly specific radiolabeling of monoclonal antibodies (mAbs) and their effect on the tumor and normal tissue uptake. Radioimmunotherapy (RIT) employs mAbs complexed into radionuclides that emit

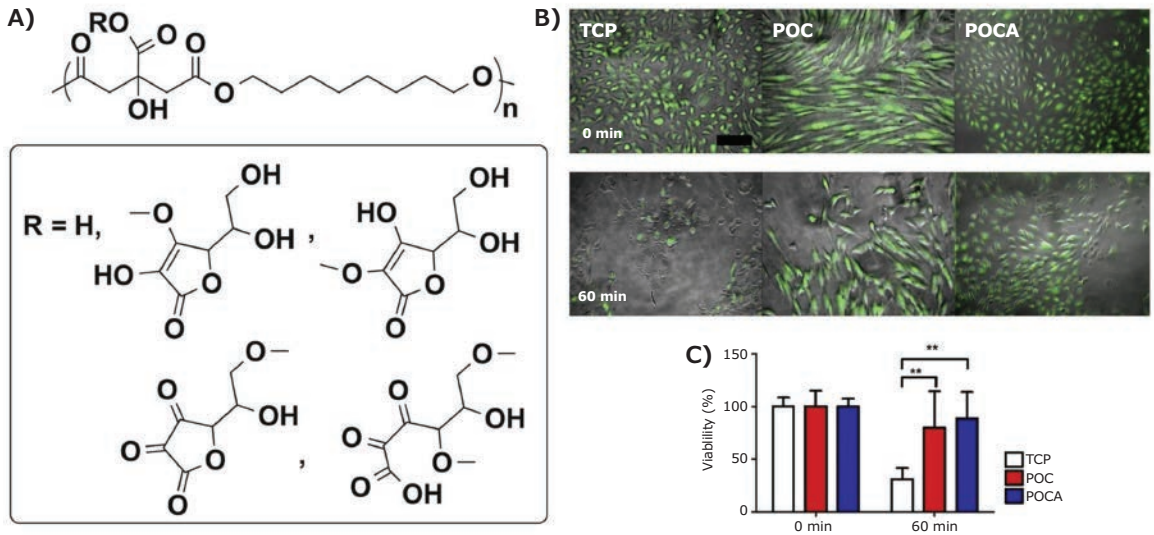

Figure 3. **A**) Proposed structure and scheme of poly(1,8-octanediol-co-citrate-co-ascorbate) (POCA). In case of R = H, the copolymer is poly(1,8-octanediol-co-citrate) (POC). **B**) Human umbilical vein endothelial cells (HUVECs) cultured on top of POC and POCA showed prolonged survival upon menadione stimulation for 60 min. POC and POCA provided protection from excessive ROS-induced cell death. Combined overlap image of contrast light microscopy with fluorescent image shown. Green indicates calcein AM stain for live cells. Bar = 200 μm. **C**) Quantification of percentage of calcein AM positive cells after 120 min relative to unchallenged cells. N = 4, Mean ± S.D., **p < 0.01. TCP stands for tissue culture plate. Reprinted with permission from reference 20, copyright 2014 American Chemical Society.

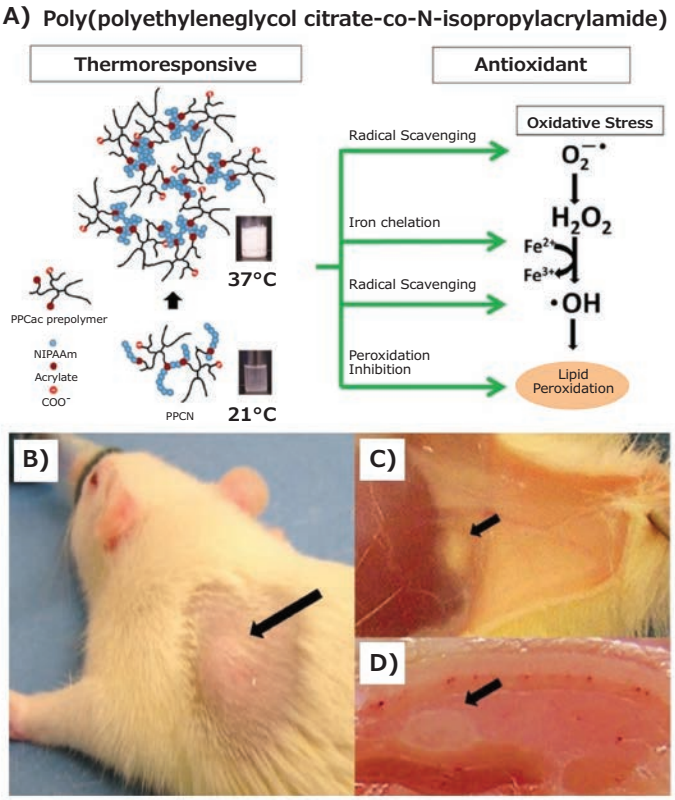

Figure 4. A) Poly(polyethylene glycol citrate-*co*-*N*-isopropylacrylamide) (PPCN) polymer gel structure. The PPCN gel has a lower critical solution temperature (LCST) of 26 °C and exhibits intrinsic antioxidant properties based on its ability to scavenge free radicals, chelate metal ions, and inhibit lipid peroxidation. Subcutaneous injection of 150 µL of PPCN (100 mg/mL, pH = 7.4) in female Sprague Dawley rats. Black arrows denote gel location **B**) directly after injection on the back of rat, a palpable lump was formed **C**) PPCN gel after 3 days **D**) frozen section of PPCN gel in tissue harvested at 30 days. Most of the gel has been replaced by new tissue. Reprinted with permission from reference 20, copyright 2014 American Chemical Society.

α-particles, β-particles, or Auger electrons for systemic radiation treatment of cancer. However, delivery and penetration barriers for radiolabeled mAbs still exist for solid tumors. One potential approach to overcome this hurdle is to increase the proportion of antibody molecules carrying a radionuclide within tumor cells or masses. Most commonly, radiolabeling is performed by conjugating chelators to the mAbs such as diethylenetriaminepentaacetic acid (DTPA) or tetraazacyclododecane-1,4,7,10-tetraacetic acid (DOTA) to form a complex with radiometals, yet with very low substitution/chelation yields. A new metal-chelating polymer, based on a polyglutamide (PGlu) backbone with grafted DOTA and polyethylene glycol (PEG), showed very effective RIT treatment of different-sized tumor deposits.[23,24]

Antioxidant Polymer Nanotherapies

As previously discussed, instead of encapsulating the antioxidants into polymer gels or nanoparticles, an alternative method offering promising new treatments is conjugating the drug or antioxidant directly to a degradable or non-degradable polymer. This approach is driven by the growing market of pharmaceutically active yet structurally fragile pro-drugs, whereby a selected functional group of the drug molecule is modified to protect from deactivation and allow for conversion back to the active form upon administration. Many medical conditions can now be treated with emerging nanotherapeutics such as thrombus, which is associated with excess formation of harmful H_2O_2.[25] Since most small molecule antioxidants possess one or more hydroxy or thiol groups, they can be functionalized and formulated into polyester, polyanhydride, or poly(β-amino ester) polymeric structures. For instance, poly(beta-amino ester) (PBAE) chemistry was employed to conjugate quercetin and curcumin into crosslinked polymer films, microparticles, nanoparticles, or nanogel systems.[26] Briefly, the polymer was synthesized by reacting acryloyl chloride and triethylamine with curcumin or quercetin, forming an intermediary acrylic. The formed acrylic reacted with PEG diacrylate (PEG400DA), a primary diamine such as 4,7,10-Trioxa-1,13-tridecane diamine (TTD), 2,20 (ethylenedioxy)-bis-ethylamine (EDBE), and hexame-thyldiamine (HMD) to form a crosslinked polymer network. The nanogels, 50 to 800 nm in size, provided uniform release over 24–36 hours by bulk hydrolytic degradation. Both curcumin and quercetin conjugated systems demonstrated protection against induced oxidative stress in endothelial cells. The curcumin PBAE nanogels were explicitly studied for their action on mitochondrial oxidative stress, a significant source of ROS and RONS production, and were found to be more effective at interrupting ROS production than free curcumin.

Enhanced bioactive antioxidant formulations are critical for the treatment of inflammatory diseases as well, such as atherosclerosis. A hallmark of early atherosclerosis is the oxidized low-density lipoprotein (oxLDL) uptake by macrophages, which results in foam cells and plaque formation in the arterial wall. A new class of nanoparticles with antioxidant polymer cores and shells comprising scavenger receptor targeting amphiphilic macromolecules based on diglycolic acid linked ferulic acid-poly(anhydride-ester) were shown to counteract the uptake of high levels of oxLDL and regulate ROS in human monocyte-derived macrophages (HMDMs).[27] A recent relevant study demonstrated a novel class of antioxidant polymer nanoparticles attenuated ultraviolet B radiation-induced skin inflammatory disorders in Kud:Hr- hairless mice. These nanoparticles were administered orally, as the technology is designated as oral nanotherapeutics.[28]

Additionally, antioxidant polymer nanoparticles made from methoxy-poly(ethylene glycol)-*b*-poly(chloromethylstyrene) (MeO-PEG-*b*-PCMS) provided an effective anti-aging strategy for the protection of the skin against ROS and the reduction of the skin-damaging effects of prolonged UV exposure. Briefly, MeO-PEG-*b*-PCMS was synthesized by the radical polymerization of chloromethylstyrene (CMS) using methoxy-poly(ethylene glycol)-hydroxyl with a grafted chain transfer agent. Subsequently, the chloromethyl groups were converted to a nitroxide radical moiety by an amination reaction with the NH_2-TEMPO radical (**Figure 5A**). This amphiphilic block copolymer was used to synthesize orally administered nanoparticles via hydrophobic interactions of the active NH_2-TEMPO segments. Upon dissociation at low pH, the redox polymer was released and circulated in the blood to provide protection against ROS.

Another promising edible antioxidant polymer that can be transformed into nanoparticles is gallic acid grafted chitosan which exhibited stronger antioxidant potential and adjustable rheological properties, than pure gallic acid.[29] Similarly, conjugating chitosan with chlorogenic acid also formed robust antioxidant polymer systems against lipid peroxidation. The copolymer demonstrated better antioxidant potential, and its capacity to inhibit β-carotene-linoleic acid bleaching and lipid peroxidation was stronger than chlorogenic acid alone.

Epigallocatechin-3-gallate (EGCG) is the most active catechin of tea polyphenols and accounts for 50–80% of the total catechin present in green tea. Potential health-promoting properties of EGCG include strong antioxidant activity, cancer chemoprevention, radioprotection, cardiovascular health improvement, and anti-obesity capabilities. EGCG was reported to be approximately 10 times as effective as β-carotene and L-ascorbate in alkyl peroxyl radical scavenging.[30] However, EGCG's bioactivity is limited by its low oral bioavailability and poor stability. EGCG is highly soluble in water; however, it can be easily oxidized in the aqueous phase. It can be grafted into proper polymer backbones to circumvent these limitations and serve as a robust theranostics polymer. To this end, β-Lactoglobulin (BLG)–chlorogenic acid (CA) conjugates with controlled grafted amounts of EGCG were generated by a free radical-induced grafting method. The resulting nanoparticles had an average size of 100 nm and encapsulated up to 75% EGCG. Their use and functionality in cancer therapeutics have yet to be researched. However, they are expected to produce promising results that could pave the way for synthesizing other functional β-Lactoglobulin-based polymer nanoparticles.

Finally, we would like to stress the importance of designing antioxidant polymers from metalloproteins (a protein that contains a metal ion cofactor) such as polymer/hemoglobin assemblies.[31] This approach is not to encapsulate hemoglobin like a drug but to form polymeric hemoglobin nanostructures that can be used to treat health problems effectively related to hypoxia, for instance. Promising strides have already been made. For example, polymeric nanoparticles obtained from hemoglobin conjugated with antioxidant enzymes via dicarboxymethylated poly(ethylene glycol) (PEG) linkers and ring opening polymerization (**Figure 6**) have shown a beneficial effect in protecting pancreatic beta cells from severe hypoxia at transplantation sites.[32] Similarly, polyhemoglobin-superoxide dismutase-catalase was designed to function as an oxygen carrier with antioxidant properties. The polymer was prepared by crosslinking hemoglobin with superoxide dismutase and catalase with glutaraldehyde. This hemoglobin polymer decreased the formation of oxygen radicals compared to hemoglobin alone in a rat intestinal ischemia-reperfusion model.[33] A novel thermo-responsive hemoglobin-polymer conjugate was also reported. The polymer was synthesized by reacting the lysine amino groups of hemoglobin and carboxyl groups of a copolymer, poly(*N*-isopropylacrylamide) grafted carboxylated dextran, via single electron transfer living radical polymerization. Upon heating above LCST, the conjugate could form isolated uniform spherical nanoparticles.[34]

Future Perspectives

Due to ongoing elucidation of the exact role of oxidative stress in a plethora of pathologies, recent polymer science research has led to a remarkable increase in studies related to oxidative stress-lowering

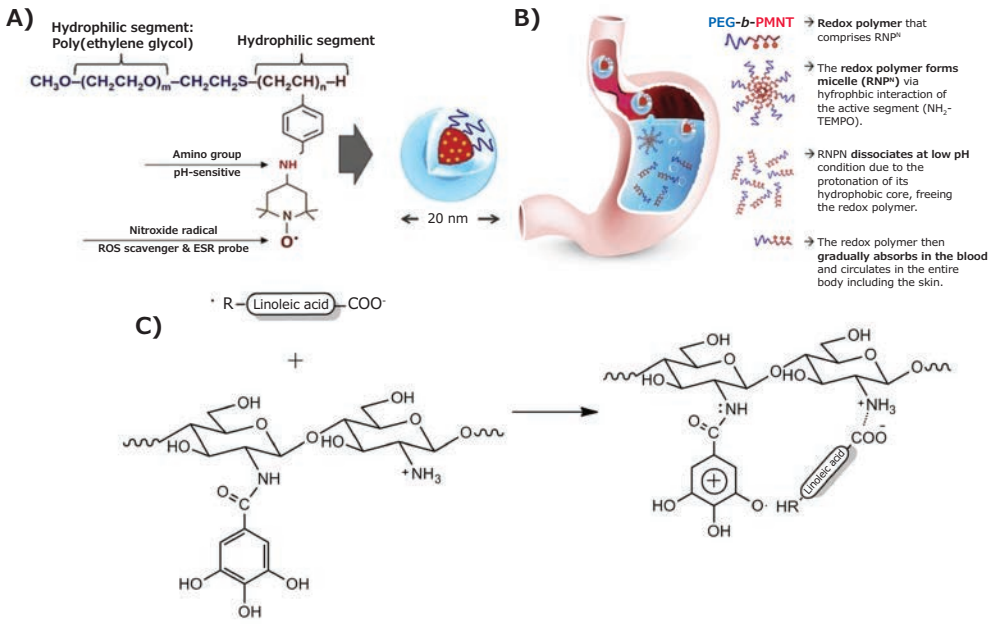

Figure 5. Design of oral nanoparticles, their delivery, and absorption in the body, including the skin. **A**) Chemical structure of the pH-sensitive polymer nanoparticles. **B**) Graphical illustration of the oral delivery of the antioxidant polymer nanoparticles and their absorption into the body and the skin area. The unique characteristics of the nanoparticles allow the gradual absorption into the bloodstream after oral administration, keeping their bioavailability high for their effective ROS scavenging effect. Reprinted with permission from reference 28, copyright 2017 Elsevier. **C**) Proposed interaction between gallic acid–chitosan and free linoleic acid radicals. Reprinted with permission from reference 29, copyright 2014 American Chemical Society.

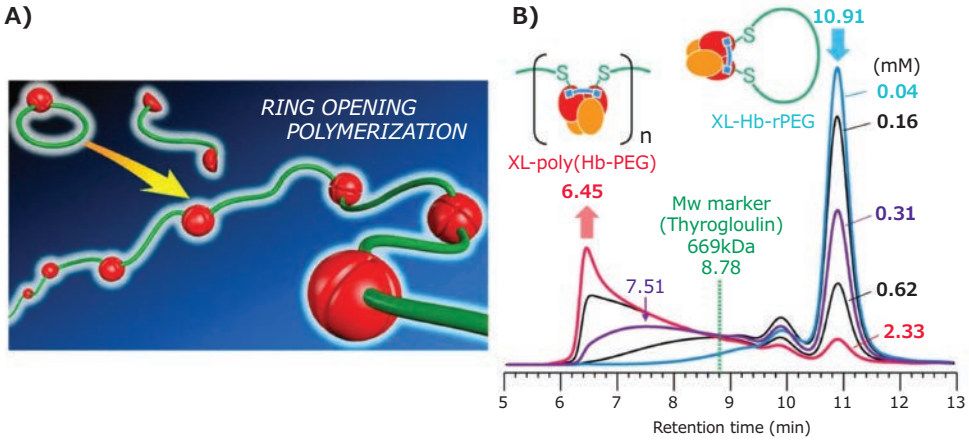

Figure 6. A) A new class of hemoglobin polymer by ring-opening polymerization. The polymer, poly(Hb–PEG), is synthesized by reacting native hemoglobin with bifunctional maleimide-PEG. The ring opening polymerization occurs by exchanging αβ subunits intermolecularly to produce poly(Hb–PEG). B) Size-exclusion chromatography (SEC) profiles obtained for products of reacting Hb-PEG monomer with bis(3,5-dibromosalicyl) fumarate (DBBF) at different monomer concentrations of 0.04, 0.16, 0.31, 0.62, and 2.33 mM. Reprinted with permission from reference 35, copyright 2019 American Chemical Society.

therapies. The main aim of this article was to demonstrate that polymeric antioxidants could be the next generation "antioxidants" in theranostics, owing to their potent antioxidant properties and increased stability in aqueous systems compared to many pure phenolic molecules. To overcome the challenges and limitations of direct, systemic administration of antioxidants, such as instability, absorption limitations, low solubility, diminished bioavailability, and the limited permeability through the cell membranes of many antioxidant molecules, polymer-based antioxidant therapies are now actively investigated. To be genuinely effective in biological applications, these polymers must be synthesized using benign methods. A deeper understanding of factors affecting antioxidant activity would provide an opportunity for the design of versatile, high-performing polymers with enhanced antioxidant activity. Since naturally occurring phenolic compounds have superior ROS scavenging profiles, these molecules can serve as excellent starting materials for synthesizing polymeric antioxidants. Enzyme catalyzed polymerization should be more studied as it enables the synthesis of polymeric phenols under environmentally friendly conditions.

Many biomedical polymers with known pro-oxidant degradation products such as polycaprolactone, polylactic acid, or polyglycolic acid should be engineered to be neutral or even antioxidant by copolymerization with antioxidants. This will enable a gradual shift from encapsulation approaches to the structural incorporation of antioxidants into the polymer system. Yet, most reports on cell viability data do not necessarily compare the measured upper limits for cell survival with the local concentrations needed for effective oxidative stress modulation. This makes it quite problematic to judge whether antioxidant polymer technologies qualify for addressing particular pathologies. At the same time, our understanding of how natural antioxidants function has improved. For instance, recent studies on the structure and antioxidant properties confirm that the antioxidant properties of flavonoids increase due to the presence of the hydroxyl group in the C3 position and the catechol moiety. In the case of kaempferol and quercetin, the 3-OH hydroxyl group is the most involved in forming a radical structure. The delocalization of electronic charge because of ligand complexing with metals of high ionic potential (Fe (III), Ln (III) Y (III)) can lead to increasing the antioxidant properties, according to our preliminary studies, even by up to 10 times. However, the positive or negative roles of these metals during theranostics applications are to be evaluated very carefully.

New polymer synthesis reports are encouraging and promising, such as electroactive and biocompatible tetra(aniline)-based terpolymers with tunable intrinsic antioxidant properties *in vivo*. These polymers are obtained from non-biodegradable or inedible compounds such as tetra(aniline), fumaryl chloride, and polyethylene glycol. However, upon polymerization transform into biodegradable and non-toxic antioxidant polymers. Cationic 1,2,3-triazole functionalized starch derivatives are promising new systems that still lack extensive medical theranostics studies. As such, future studies should take into account (i) analyzing the impact of prolonged exposure to various level concentrations of polymer (nano) antioxidants; (ii) assessing the potential risks during fabrication, manipulation, and storage; (iii) simplifying the fabrication processes for the manufacture of highly potent systems; (iv) enhancing the reproducibility, biocompatibility, reliability, robustness, and stability of polymer (nano) antioxidants in biological microenvironments; and (v) designing microreactors that can effectively control the parameters of reaction synthesis.

Polymeric antioxidants have exhibited high potency for oxidative stress depletion with high cellular antioxidant potential, specificity, and targeted delivery. However, to achieve significant clinical benefits, a thorough understanding of the detailed antioxidative mechanisms of these new polymers necessitates extensive cross-collaboration of experts from various fields, including materials science, chemistry, and physical and biomedical fields. In-depth mechanistic studies of oxidative stress *in vivo* will be helpful in revolutionizing the polymer antioxidant therapeutic field.

References

(1) Fuchs-Tarlovsky, V. *Nutrition* **2013**, *29* (1), 15–21.
(2) Ferdous, U. T.; Yusof, Z. N. B. *Front. Pharmacol.* **2021** *12*, 157.
(3) Yeo, J.; Lee, J.; Lee, S.; Kim, W. J. *Adv. Ther.* **2021**, *4* (4), 2000270.
(4) Maraveas, C.; Bayer, I. S.; Bartzanas, T. *Polymers* **2021**, *13* (15), 2465.
(5) He, X.; Liu, G.; Tian, Y.; Mao, T.; Wu, H.; Wei, Y.; Tao, L. *Macromol. Biosci.* **2020**, *20* (12), 1900419.
(6) Spizzirri, U. G.; Iemma, F.; Puoci, F.; Cirillo, G.; Curcio, M.; Parisi, O. I.; Picci, N. *Biomacromolecules* **2009**, *10* (7), 1923–1930.
(7) Zhang, G.; Nam, C.; Chung, T. M.; Petersson, L.; Hillborg, H. (2017). *Macromolecules* **2017**, *50* (18), 7041–7051.
(8) Vilela, C.; Pinto, R. J.; Coelho, J.; Domingues, M. R.; Daina, S.; Sadocco, P.; Freire, C. S; *et al. Food Hydrocoll.* **2017**, *73*, 120–128.
(9) Wu, W.; Pu, Y.; Shi, J. *J. Nanobiotechnol.* **2022**, *20* (1), 1–21.
(10) Tomadoni, B.; Ponce, A. ; Pereda, M.; Ansorena, M. R. *Polym. Test.* **2019**, *78*, 105935.
(11) Reano, A. F.; Pion, F.; Domenek, S.; Ducrot, P. H.; Allais, F. *Green Chem.* **2016**, *18* (11), 3334–3345.
(12) Barthomeuf, C. M.; Debiton, E.; Barbakadze, V. V.; Kemertelidze, E. P. *J. Agric. Food Chem.* **2001**, *49* (8), 3942–3946.
(13) Clemente, S. M.; Martínez-Costa, O. H.; Monsalve, M.; Samhan-Arias, A. K. *Molecules* **2020**, *25* (21), 5144.
(14) Kang, C.; Cho, W.; Park, M.; Kim, J.; Park, S.; Shin, D.; Lee, D.; *et al. Biomaterials* **2016**, *85*, 195–203.
(15) Arya, S. S.; Rookes, J. E.; Cahill, D. M.; Lenka, S. K. *Adv. Tradit. Med.* **2021**, *21* (3), 1–17.
(16) van Lith, R.; Ameer, G. A. Antioxidant polymers as biomaterial. In *Oxidative Stress and Biomaterials,* Academic Press, 2016; pp 251–296.
(17) Fattahi, A.; Golozar, M. A.; Varshosaz, J.; Sadeghi, H. M.; Fathi, M. *Carbohydr. Polym.* **2012**, *87* (2), 1176–1184.
(18) Wattamwar, P. P.; Mo, Y.; Wan, R.; Palli, R.; Zhang, Q., Dziubla, T. D. *Adv. Funct. Mater.* **2010**, *20* (1), 147–154.
(19) van Lith, R.; Gregory, E. K.; Yang, J.; Kibbe, M. R.; Ameer, G. A. *Biomaterials* **2014**, *35* (28), 8113–8122.
(20) Yang, J.; Van Lith, R.; Baler, K.; Hoshi, R. A.; Ameer, G. A. *Biomacromolecules* **2014**, *15* (11), 3942–3952.
(21) Imran ul-haq, M.; Hamilton, J. L.; Lai, B. F.; Shenoi, R. A.; Horte, S.; Constantinescu, I.; Kizhakkedathu, J. N., *et al. ACS Nano* **2013**, *7* (12), 10704–10716.
(22) Zhou, T.; Neubert, H.; Liu, D. Y.; Liu, Z. D.; Ma, Y. M.; Kong, X. L.; Hider, R. C.; *et al. J. Med. Chem.* **2006**, *49* (14), 4171–4182.
(23) Aghevlian, S.; Lu, Y.; Winnik, M. A.; Hedley, D. W.; Reilly, R. M. *Mol. Pharm.* **2018**, *15* (3), 1150–1159.
(24) Liu, P.; Boyle, A. J.; Lu, Y.; Adams, J.; Chi, Y.; Reilly, R. M.; Winnik, M. A. *Biomacromolecules* **2015**, *16* (11), 3613–3623.
(25) Zhao, Z.; Yang, F.; Zhang, X.; Sun, J.; He, Z.; Luo, C. *Biomaterials* **2020**, *255*, 120200.
(26) Wattamwar, P. P.; Biswal, D.; Cochran, D. B.; Lyvers, A. C.; Eitel, R. E.; Anderson, K. W.; Dziubla, T. D.; *et al. Acta Biomater.* **2012**, *8* (7), 2529–2537.
(27) Chmielowski, R. A.; Abdelhamid, D. S.; Faig, J. J.; Petersen, L. K.; Gardner, C. R.; Uhrich, K. E.; Moghe, P. V.; *et al. Acta Biomater.* **2017**, *57*, 85–94.
(28) Feliciano, C. P.; Nagasaki, Y. *Biomaterials* **2017**, *142*, 162–170.
(29) Xie, M.; Hu, B.; Wang, Y.; Zeng, X. *J. Agric. Food Chem.* **2014**, *62* (37), 9128–9136.
(30) Fan, Y.; Zhang, Y.; Yokoyama, W.; Yi, J. *RSC Adv.* **2017**, *7* (35), 21366–21374.
(31) Jansman, M. M.; Hosta-Rigau, L. *Adv. Colloid Interface Sci.* **2017**, *260*, 65–84.
(32) Nadithe, V.; Bae, Y. H. *Tissue Eng. Part A* **2011**, *17* (19–20), 2453–2462.
(33) D'Agnillo, F.; Chang, T. *Nat. Biotechnol.* **1998**, *16* (7), 667–671.
(34) Wang, S.; Yuan, F.; Chen, G.; Tu, K.; Wang, H.; Wang, L. Q. *RSC Adv.* **2014**, *4* (95), 52940–52948.
(35) Matsuhira, T.; Yamamoto, K.; Sakai, H. *Biomacromolecules* **2019**, *20* (4), 1592–1602.

Stimuli-responsive Materials

Name	Description	Molecular Weight (Average M_n)	Cat. No.
Poly(*N*-isopropylacrylamide)	powder or crystals	~40,000	**535311-10G**
Poly(*N*-isopropylacrylamide) triethoxysilane terminated	solid	5,000	**760978-1G** **760978-5G**
Poly(*N*-isopropylacrylamide), amine terminated	solid	2,500	**724823-1G** **724823-5G**
	solid	5,500	**724831-1G** **724831-5G**
Poly(*N*-isopropylacrylamide), carboxylic acid terminated	powder	2,000	**724815-1G** **724815-5G**
	powder	5,000	**724807-1G** **724807-5G**
	powder	7,000	**724866-1G** **724866-5G**
	powder	10,000	**724459-5G**
Poly(*N*-isopropylacrylamide), *N*-hydroxysuccinimide (NHS) ester terminated	powder	2,000	**725668-1G** **725668-5G**
Poly(*N*-isopropylacrylamide-*co*-acrylamide)	powder acrylamide, 15 mol %	22,500	**738735-5G**
Poly(*N*-isopropylacrylamide-*co*-butylacrylate)	solid butylacrylate, 5 mol %	30,000	**762857-5G**
	solid butylacrylate, 12 mol %	30,000	**762881-5G**
Poly(*N*-isopropylacrylamide-*co*-methacrylic acid)	powder methacrylic acid, 5 mol %	50,000	**724467-5G**
	solid methacrylic acid, 10 mol %	60,000	**724858-5G**
Redox responsive poly(ethylene glycol)-*block*-poly(ε-caprolactone)	solid, powder, chunks, or granules	PCL M_n 15,000 PEG average M_n 5,000	**925624-1G**
Redox responsive poly(ethylene glycol)-*block*-poly(lactide-*alt*-glycolide)	powder, chunks, or granules	PLGA M_n 15000 PEG average M_n 5000	**926248-1G**

Biodegradable Polymers

Name	Form	Molecular Weight	Cat. No.
Poly(D,L-lactide-*co*-glycolide)	amorphous	M_w 50,000-75,000	**430471-1G** **430471-5G**
Polyglycolide	solid	viscosity 1.1-1.7 dL/g, 0.1 % (w/v) in hexafluoroisopropanol	**457620-1G** **457620-5G** **457620-10G**
Polylactide-block-poly(ethylene glycol)-*block*-polylactide	solid	average M_n (1,500-900-1,500) PEG average M_n 900 PLA average M_n 1,500	**659630-1G**
Polylactide-block-poly(ethylene glycol)-*block*-polylactide	solid	average M_n (1,000-10,000-1,000) PEG average Mn 10,000 PLA average Mn 1,000	**659649-1G**
Resomer® X 206 S, poly(dioxanone)	solid	viscosity 1.5-2.2 dL/g, 0.1 % (w/v) in hexafluoroisopropanol	**719846-1G** **719846-5G**
Resomer® L 206 S, Poly(L-lactide), ester terminated	granular	viscosity 0.8-1.2 dL/g, 0.1 % in chloroform	**719854-5G** **719854-25G**
Resomer® RG 653 H, Poly(D,L-lactide-*co*-glycolide)	amorphous	M_w 24,000-38,000	**719862-1G** **719862-5G**
Resomer® RG 503 H, Poly(D,L-lactide-*co*-glycolide)	amorphous	M_w 24,000-38,000	**719870-1G** **719870-5G**
Resomer® RG 502, Poly(D,L-Lactide-*co*-Glycolide)	amorphous	M_w 7,000-17,000	**719889-1G** **719889-5G**
Resomer® RG 502 H, Poly(D,L-lactide-*co*-glycolide)	amorphous	M_w 7,000-17,000	**719897-1G** **719897-5G**
Resomer® RG 504 H, Poly(D,L-lactide-*co*-glycolide)	amorphous	M_w 38,000-54,000	**719900-1G** **719900-5G**
Resomer® RG 752 H, Poly(D,L-lactide-*co*-glycolide)	amorphous	M_w 4,000-15,000	**719919-1G** **719919-5G**
Resomer®) RG 756 S, Poly(D,L-lactide-*co*-glycolide)	amorphous	M_w 76,000-115,000	**719927-1G** **719927-5G**
Resomer® R 203 S, Poly(D,L-lactide)	amorphous	M_w 18,000-28,000	**719935-1G** **719935-5G**
Resomer® R 203 H, Poly(D,L-lactide)	amorphous	M_w 18,000-24,000	**719943-1G** **719943-5G**
Resomer® R 202 S, Poly(D,L-lactide)	amorphous	M_w 10,000-18,000	**719951-1G** **719951-5G**
Resomer® R 202 H, Poly(D,L-lactide)	amorphous	M_w 10,000-18,000	**719978-1G** **719978-5G**
Resomer® RG 504, Poly(D,L-lactide-*co*-glycolide)	amorphous	M_w 38,000-54,000	**739944-1G** **739944-5G**
Resomer® RG 503, Poly(D,L-lactide-*co*-glycolide)	amorphous	M_w 24,000-38,000	**739952-1G** **739952-5G**
Resomer® RG 505, Poly(D,L-lactide-*co*-glycolide)	amorphous	M_w 54,000-69,000	**739960-1G** **739960-5G**
Resomer(R) RG 858 S, Poly(D,L-lactide-*co*-glycolide)	amorphous	M_w 190,000-240,000	**739979-1G** **739979-5G**
Poly(L-lactide)	solid	M_w ~260,000	**81273-10G**
	solid	M_n 59,000 M_w 101,000	**93578-5G-F**
	solid	average Mn 40,000	**94829-1G-F** **94829-5G-F**
	solid	M_n 103,000 M_w 259,000	**95468-1G-F** **95468-5G-F**

MERCK

IMPROVE DELIVERY

A Step-by-Step Guide

Low drug solubility and stability often reduce the effectiveness of an otherwise promising therapeutic candidate. In this comprehensive guide, you'll discover how polymers can provide the drug delivery solutions you need for controlled release, targeting, and solubility enhancement.

Request your copy online at:
SigmaAldrich.com/ddtechnique

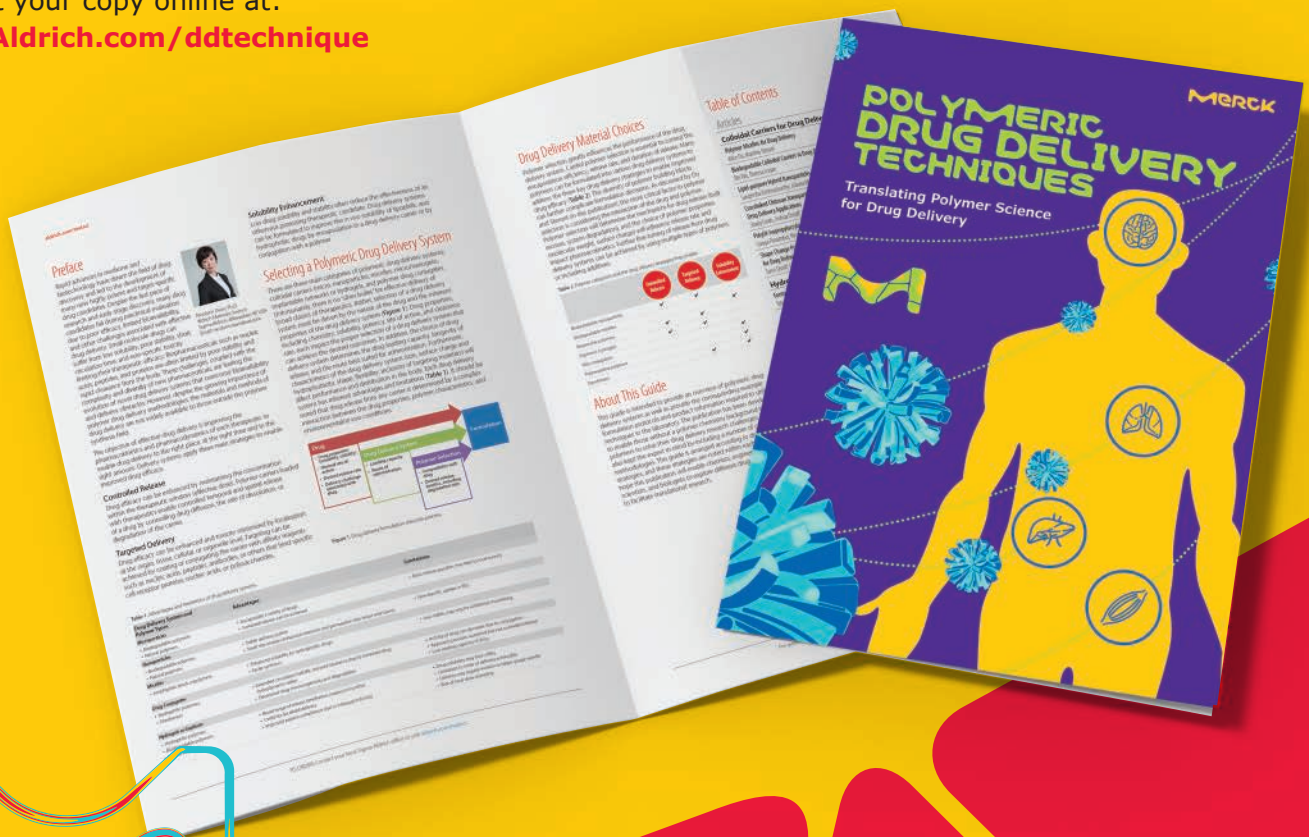

Therapeutic Nanoparticles Harness Myeloid Cells for Brain Tumor-targeted Delivery and Immunomodulation


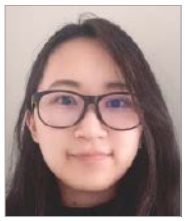


Abby Ellingwood,[1#] Hanxiao Wan,[1#] Catalina Lee-Chang,[1] Maciej S. Lesniak,[1*] Peng Zhang[1*]

[1] Department of Neurosurgery, Lou and Jean Malnati Brain Tumor Institute, Robert H. Lurie Comprehensive Cancer Center, Northwestern University Feinberg School of Medicine, Chicago, IL, USA
[#] These authors contributed equally to this work.
[*] Email: maciej.lesniak@northwestern.edu and peng@northwestern.edu

Introduction

The full potential of therapeutics for glioblastoma (GBM), the most aggressive and deadliest brain malignancy in adults, has yet to be reached. Malignant brain tumors have been well-characterized as immunologically cold, as defined by massive infiltration of immunosuppressive tumor-associated myeloid cells (TAMCs) unrivaled by any other types of solid tumors.[1] TAMCs are a heterogeneous population of myeloid-derived immunosuppressive cells, including myeloid-derived suppressor cells (MDSCs), tumor-associated macrophages (TAMs), and neutrophils. As a hallmark of GBM, TAMCs represent the predominant immune cell population, comprising up to 80% of the leukocytes in the brain tumor microenvironment.[2,3] This unique TAMC-rich immune microenvironment is responsible for GBM resistance to emerging immunotherapies and existing standard of care treatments, such as chemotherapy and radiotherapy. The central role of TAMCs in brain tumor progression and therapeutic resistance has led to identifying the myeloid compartment as a promising therapeutic target for GBM.

This mini-review highlights recent progress in implementing nanotechnology in advancing TAMC-targeted therapies for GBM. One significant advantage of nanotechnology-mediated therapy is its versatility in encapsulating therapeutics with diverse physiochemical and/or pharmacological properties to overcome the challenges encountered through *in vivo* applications. These issues could be further solved by utilizing targeting mechanisms to enable precision therapeutic delivery to the organs/cells of interest. In addition, dual-/multi-functional nanoparticles that exert biological/pharmacological activities alone have also been discovered. Because TAMCs massively infiltrate into brain tumors and play a key role in causing immunosuppression-related therapy resistance of GBM, this review will be focused on two nanotherapeutic approaches that have been developed for harnessing TAMCs for GBM therapy, i.e., (i) immunomodulation of TAMCs to activate antitumor immune responses, and (ii) hijacking TAMCs as cellular carriers for GBM-targeted drug delivery.

Nanotherapeutic Targeting of TAMCs for GBM Immunomodulation

Recent discoveries revealing the immunological composition of the tumor microenvironment and the crosstalk between tumor and tumor-associated immune cells have identified the predominance of the myeloid compartment in GBM and its central role in affecting GBM progression and therapy outcome. Within the GBM microenvironment, TAMCs are programmed by tumor cells to exhibit a tumor-supporting, immunosuppressive (typically classified as M2 or M2-like) phenotype, which potently suppresses the antitumor activity of effector T cells, induces regulatory T and B cells, and supports tumor progression, migration, and therapy resistance.[4] Therefore, therapeutic targeting of TAMCs to blunt their tumor-supportive activities and/or reinforce their intrinsic antitumor, proinflammatory immune activities is a promising immunotherapy branch that could work alone or synergistically improve existing treatments for GBM.

Targeting strategies for therapeutic delivery to TAMCs

Precision targeting of TAMCs is challenging due to the high heterogeneity of the GBM microenvironment as well as the phenotypic plasticity of TAMCs. To overcome these obstacles, novel targeting strategies have been studied through the rational design of multifunctional nanomaterials with surface-decoration of targeting ligands that exhibit high binding affinity with overexpressed receptors on TAMCs. For example, to enable a robust genetic modulation of M2 TAMs, Stephan et al. chemically modified their poly (β-amino ester) (PbAE)-based nanoparticles with an α-D-mannopyranosyl-(1→2)-α-D-mannopyranose (Di-mannose) ligand through a polyglutamic acid (PGA) linker (**Figure 1A**).[5] Di-mannose is a targeting ligand with high binding affinity to macrophage mannose receptor 1 (mrc1 or CD206) that are overexpressed on M2 TAMs. In addition to its role as a TAM-targeting ligand, Di-mannose also stabilized the nanoparticle by shielding the excess positive charge of the PbAE polymers post-mRNA encapsulation, which significantly reduced the nonspecific binding of nanoparticles to non-targeted cells through charge-charge interactions. As a result, substantial transfection of the mRNA therapeutics in TAMs was achieved using

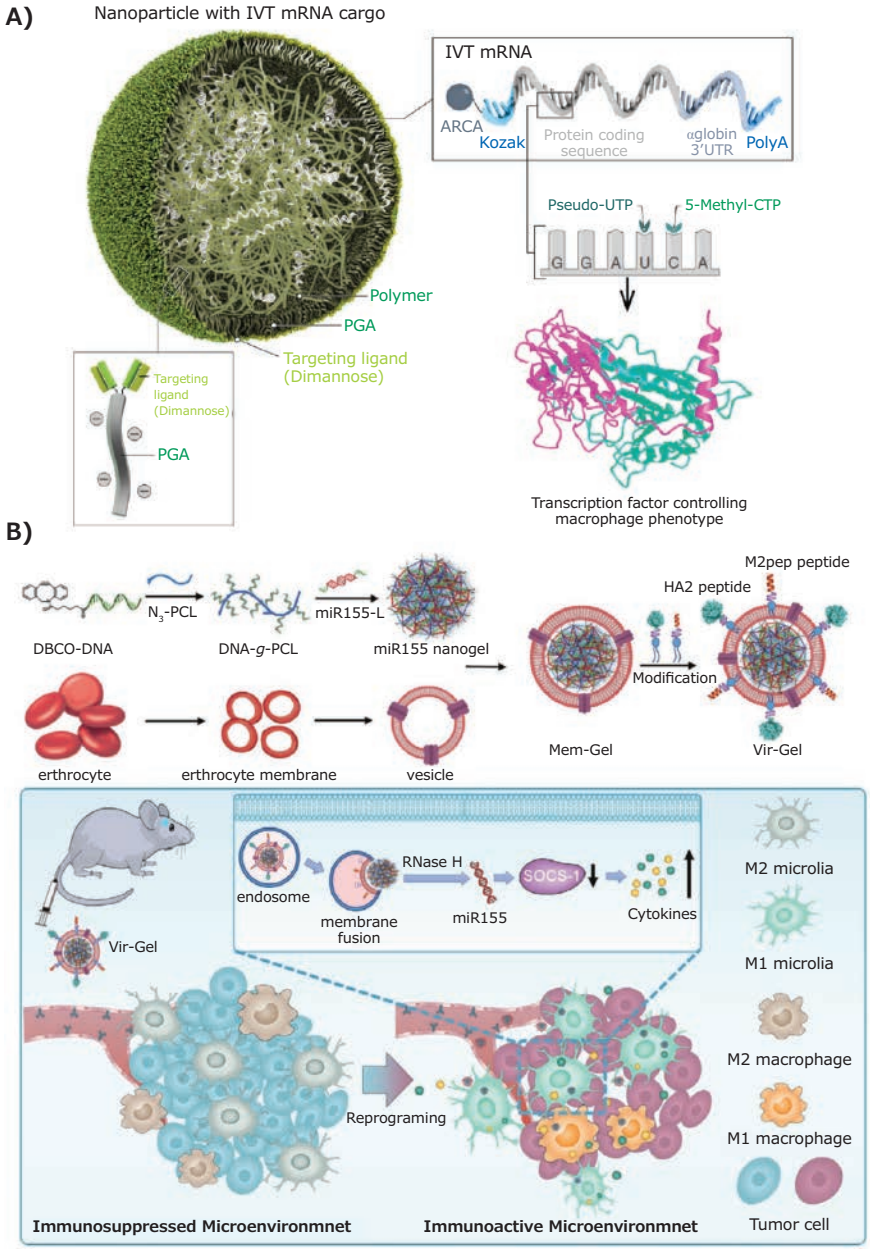

Figure 1. Ligand-receptor interaction-mediated nanoparticle targeting of tumor-associated macrophages. **A**) Schematic representation of M2 macrophage-targeting nanoparticles through binding to mannose receptor. Reproduced from reference 5, copyright 2019 Springer Nature. Open access article distributed under the terms of the Creative Commons CC BY license. **B**) Design of a dual-peptide modified, erythrocyte membrane-coated virus-mimicking nanogel for miRNA delivery. Reproduced with permission from reference 6, copyright 2021 John Wiley and Sons.

these TAM-targeting nanoparticles. Another cutting-edge TAM-targeting strategy by the Zhang group involves a dual-peptide functionalization of nanogels to target the miRNA-loading nanogel towards M2 TAMs and microglia in GBM by mimicking the process of virus infection (**Figure 1B**).[6] Two functional peptides, M2pep and HA2, were covalently conjugated to the terminal maleimide group of 1,2-distearoylsn-glycero-3-phosphoethanolamine-*N*-[maleimide(polyethylene glycol)-2000] (DSPE-PEG-Mal), and then inserted into the membrane of the nanogel formed by DNA-grafted polycaprolactone (DNA-*g*-PCL). These peptides played distinct roles in regulating the cellular uptake of the nanogel and drug release profiles. M2pep peptide was initially discovered through phage display[7] and utilized as a targeting ligand to enhance the nanogel uptake by M2 immunosuppressive microglia and macrophage. In contrast, the function of influenza virus-derived HA2 peptide was shown to trigger drug release through an increased fusion of nanogel with the endosomal membrane.

Besides targeting M2 TAMs, tremendous research efforts have also been put into creating innovative approaches that simultaneously enable efficacious therapeutic delivery to a heterogeneous population of immunosuppressive myeloid cells. Research findings from the Lesniak group have indicated that programmed death-ligand 1 (PD-L1) is overexpressed in different subsets of TAMCs in GBM models over other immune cell populations and tumor cells, and accordingly demonstrate the use of anti-PD-L1 therapeutic antibodies for functionalizing and targeting lipid nanoparticles to TAMCs.[8] Despite being a standard of care treatment for newly diagnosed GBM, radiotherapy upregulated PD-L1 expression in TAMCs, thus potentiating the targeting and delivery efficiency of these nanoparticles. This is among the first studies to demonstrate the utility of PD-L1 as a targeting moiety for the delivery of therapy rather than solely as an immune checkpoint inhibitor. Similarly, Huang et al. have explored the possibility of using an innovative "three-birds-one-stone" multi-targeting strategy.[9] An α7 nicotinic acetylcholine receptors (nAChRs)-binding peptide, ^{D}CDX (CGREIRTGRAERWSEKF), was utilized to functionalize a liposomal nanoparticle formulation for simultaneous drug delivery to multiple cell types that overexpress the same receptor nAChRs, including TAM, glioma, and glioma vessel endothelium. Their imaging results indicate a much-enhanced BBB-penetrating efficiency and brain tumor-specific accumulation of the peptide-functionalized liposomes.

Nanoparticle-enabled Immunomodulation of TAMCs

TAMCs plasticity enables the diverse functionality of these innate immune cells and therefore their multifaceted roles in the GBM microenvironment. TAMCs could either exhibit an immunosuppressive or anti-inflammatory (typically classified as M2-like or alternative) phenotype or an immunostimulatory or proinflammatory (typically classified as M1-like or classical) phenotype. Consequently, TAMC-targeted therapy in cancer treatment has emphasized how to blunt the immunosuppressive functions of TAMCs and/or how to induce their antitumor activities through triggered repolarization. Including but not limited to the abovementioned TAMC-targeting efficiency, nanomedicine approaches have exhibited undoubted advantages in immunomodulation of TAMC functionality over using free therapeutics.

One significant advantage of nanotechnology-mediated drug delivery is that nanoparticles are a versatile platform capable of encapsulating and delivering different types of therapeutics to overcome the challenges that therapeutic molecules encounter upon transition to *in vivo* applications, including insufficient solubility, stability, *in vivo* circulation, tumor-specific accumulation, cell uptake, and/or therapeutic efficacy.[10] This is particularly true for nucleic acid therapeutics, whose clinical transition has been greatly limited by their unfavorable physiochemical properties.[11] To address such issues, Zhang et al. have demonstrated that their virus-mimicking nanogel carried miR155, a micro-RNA therapeutic that inhibits the expression of anti-inflammatory factor suppressor of cytokine signaling 1 (SOCS-1), whereby inducing proinflammatory cytokine production in TAMCs.[6] The nanogel was formulated by a DNA-grafted polycaprolactone (DNA-*g*-PCL) polymer, capable of encapsulating miRNA molecules through crosslinking, and coated by an erythrocyte membrane to provide additional protection to the loaded miRNA therapeutics and to increase *in vivo* brain tumor accumulation (**Figure 1B**). Accordingly, the nanogel significantly extended the miRNA lifetime *in vivo* and, combined with the peptide modification as abovementioned, improved its myeloid cell-targeting and uptake efficiency (**Figure 2A**), which led to effective repolarization of the M2-like immunosuppressive TAMs and microglia to an M1 phenotype. Another example of nanoparticle-enabled TAM-targeted delivery of nucleic acid therapeutics was reported by the Stephan group.[5] mRNA therapeutics encoding interferon regulatory factor 5 (IRF5) together with IKKβ, an IRF5-phosphorylating/activating kinase, were generated for repolarization of M2 macrophages. The mRNAs were encapsulated through charge-charge interactions with nanoparticles formed by cationic PbAE polymers. The IRF5/IKKβ mRNA nanoparticle treatment impaired immunosuppressive activity of M2 TAMs. Brain tumor regression was observed in tumor-bearing animals when mRNA nanoparticle treatment was combined with radiation (**Figure 2B**), suggesting the potential use of TAM-targeted therapy in combination therapy for GBM. Extending this line of thought, nanoparticles have also been widely used in combination therapy based on their capability to simultaneously co-deliver multiple therapeutics with distinct physiochemical and pharmacokinetic properties to ensure maximized synergistic effects. For example, Huang et al. developed a brain-targeted liposomal formulation for the co-delivery of honokiol combined with disulfiram/copper to synergistically target the mammalian target of rapamycin (mTOR) pathway in the GBM microenvironment.[9] Using blood-brain barrier (BBB)-penetrating liposomes in GBM models reshaped the mTOR-mediated glucose metabolism and boosted the antitumor immune system by activating antitumor M1 macrophage and dendritic cells and priming effector T and NK cells.

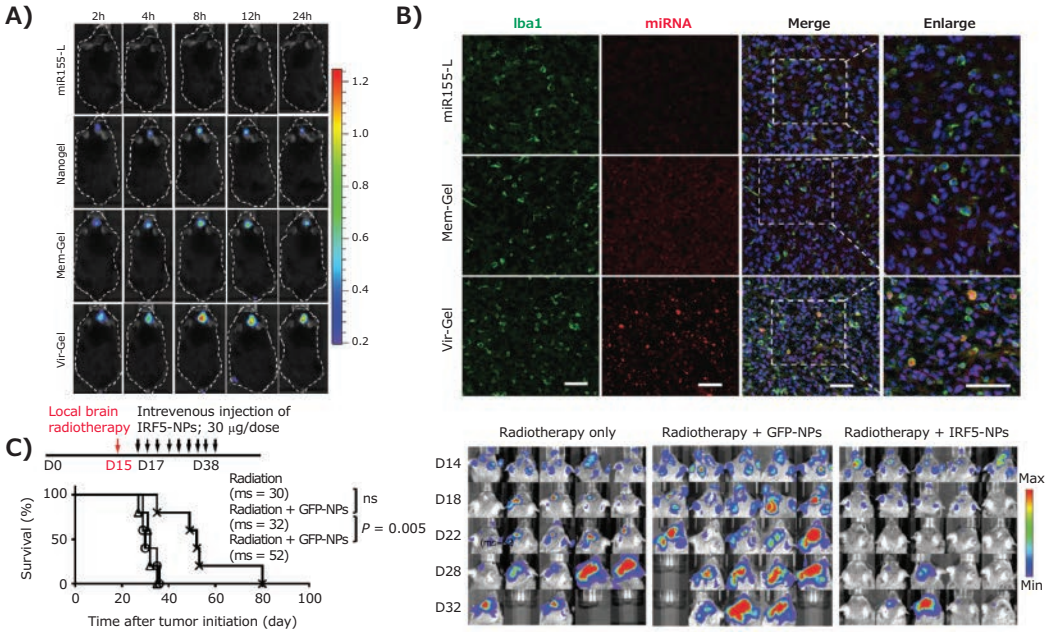

Figure 2. Macrophage-targeting nanoparticles stimulate anti-GBM immunity and prolong survival of GBM-bearing mice. A) *In vivo* fluorescence imaging and confocal laser scanning microscopy imaging indicates enhanced brain distribution and macrophage/microglia uptake of miRNA in the brain through virus-mimic nanoparticle-mediated delivery post-intravenous injection. Reproduced with permission from reference 6, copyright 2021 John Wiley and Sons. B) Kaplan-Meier animal survival curves and sequential bioluminescence imaging of brain tumors indicate the therapy efficacy of IRF5-inducing nanoparticles when combined with radiotherapy. Reproduced from reference 5, copyright 2019 Springer Nature. Open access article distributed under the terms of the Creative Commons CC BY license.

Other than an effective drug delivery carrier, dual-functional therapeutic nanoparticles that exert biological activities alone have also been developed as synergistic combinations to enhance the efficacy of their cargo.[12] The Lesniak group has recently engineered a TAMC-targeting lipid nanoparticle by functionalizing nanoparticles with an anti-PD-L1 antibody.[8] The use of this lipid nanoparticle to deliver a CDK (cyclin-dependent kinase) inhibitor effectively inhibited the interferon-gamma (IFNγ)-stimulated de novo production of PD-L1 in TAMCs, which impaired the immunosuppressive activity of TAMCs in the GBM microenvironment. In addition to a drug carrier to enable the TAMC-targeted delivery of CDK inhibitor, the nanoparticles alone induced lysosomal degradation of existing PD-L1 in TAMCs, which served as an additional mechanism to synergize with the CDK inhibitor for the PD-L1 blockade. Another study by the Lesniak group demonstrates the repolarization effects of magnetic zinc-doped iron oxide nanoparticles on MDSCs, which sensitized GBM-bearing mice to radiation therapy.[13] These solid nanoparticles coated with a cationic polymer, polyethylenimine (PEI), were efficiently taken up by MDSCs in GBM, which triggered a proinflammatory-like polarization of immunosuppressive MDSCs, as evidenced by increased expression of M1-associated genes, such as inducible nitric oxide synthase (iNOS) and tumor necrosis factor α (TNFα), and decreased M2-associated genes Arginase (Arg1) and IL10.

Harnessing GBM-infiltrating TAMCs as Cellular Carriers for Nanoparticle Delivery

Inefficient delivery of therapeutics to brain tumors remains a significant hurdle to efficacious GBM treatments. The substantial physiological barriers and pathological characteristics of GBM significantly limit sufficient drug distribution to the tumor bed.[14] To overcome such obstacles, the use of endogenous cells as cellular carriers has emerged as a promising strategy to enable efficient brain tumor-targeted delivery of therapeutics. As a hallmark of GBM, TAMCs are primarily recruited and have an intrinsic capability to overcome the biological barriers and migrate deep into the tumor mass. Thus, harnessing GBM-infiltrating myeloid cells as cellular carriers, or cellular "Trojan Horses", to enhance GBM-targeted nanoparticle delivery has captured tremendous research interest (**Figure 3**).

Macrophage-mediated Nanoparticle Delivery

Macrophages are one of the most widely studied cellular carriers for loading large amounts of nanoparticle/drug complexes. In addition to the tumor-homing efficiency, the inherent phagocytic activity of macrophages also makes such cells an ideal candidate as cellular "Trojan Horses" for nanoparticle delivery. However, rational design of nanoparticle formulations that ensure the stability of nanoparticles during migration and avoid premature drug release and unwanted toxicity to carrier cells is highly desired. To address this issue, Xie et al. constructed a nanocapsule with a core nanocomplex formed by silica and doxorubicin (Dox), a first-line chemotherapeutic reagent, through electrostatic interaction. The nanocapsule core was further protected by a solid silica sheath to reduce the premature release of Dox.[15] The thicknesses of the silica coating were optimized for extended drug release to attenuate the potential Dox toxicity to macrophages after the engulfment of the nanocapsule. A high drug loading

capacity of 16.6 pg Dox/cell and two-phase drug release kinetics were achieved without affecting cell function. After intravenous injection, macrophages effectively maintained the intracellular nanocapsule and their tumor-homing ability (**Figure 4**), which largely induced tumor cell apoptosis and contributed to suppressed tumor growth *in vivo*.

To take full advantage of macrophages as carriers for nanoparticle delivery, some research groups have paid attention to the impact of macrophage plasticity on macrophage-mediated delivery efficiency. Wang et al. have reported the use of M1-polarized macrophages to deliver Dox-loaded poly(lactide-*co*-glycolide) (PLGA) nanoparticles.[16] They indicated that M1 macrophages exhibited enhanced phagocytic capability and thus were more efficient in engulfing large amounts of nanoparticles. Moreover, the antitumor activity of M1 macrophages may add more value to the therapy with the potential to synergistically inhibit tumor growth. The results demonstrated that the PLGA nanoparticles mainly resided in the lysosome of bone marrow-derived M1 macrophages. This system showed good tumor targeting capability when injected intravenously in a U87 nude mice model.

It is worth noting that, instead of using live cells, some efforts have been put into improving nanoparticle delivery by decorating nanoparticles with the ligands originally expressed on the macrophage cell membrane to enhance tumor cell binding/uptake. For instance, when delivered by oligopeptide hydrogel together with C-X-C motif chemokine ligand 10 (CXCL10),[17]

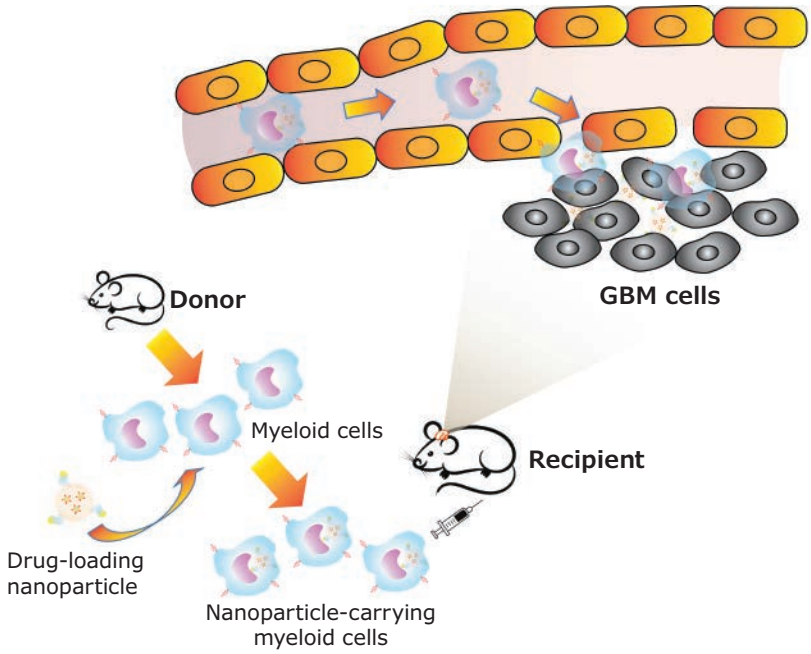

Figure 3. Schematic illustration of harnessing GBM-infiltrating myeloid cells as cellular "Trojan horse" for brain-targeted nanoparticle delivery. Drug-encapsulated nanoparticles are engulfed by myeloid cells isolated from donor mice and injected into GBM-bearing recipient mice intravenously. Upon reaching brain tumors through myeloid migration, nanoparticle/drug are released from cellular carriers to tumor cells/tumor microenvironment for antitumor effects.

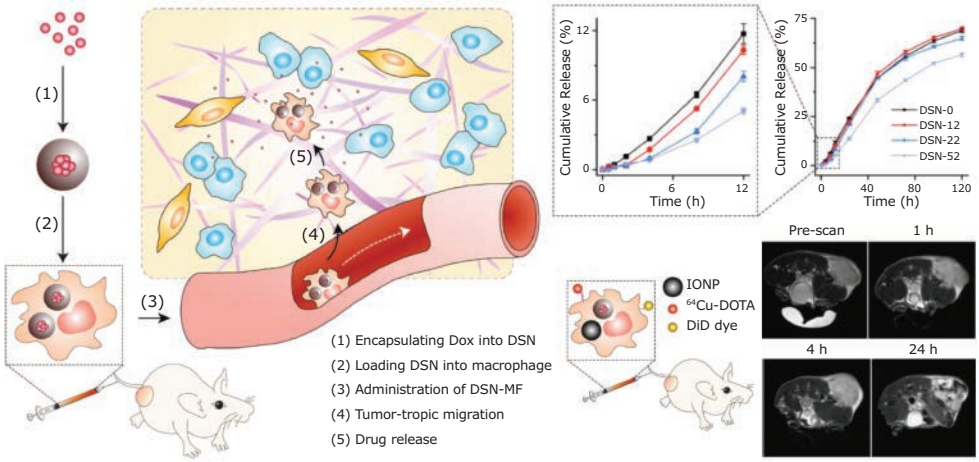

Figure 4. Schematic representation of harnessing macrophages as cellular carrier for GBM-targeted delivery. The silica matrix and coating of nanoparticle led to a controlled two-phase drug release of doxorubicin. Axial T_2 MR images indicate a tumor-targeting capability *in vivo*. Reproduced with permission from reference 15, copyright 2018 John Wiley and Sons.

α4β1 integrin, a ligand that directs the migration of glioma-associated macrophages (GAM) towards brain tumor cells, was used as camouflage to improve GBM cell uptake of a tumor-homing immune nanoregulator (THINR). This nanoregulator was synthesized by co-loading of mitoxantrone (MIT) and siRNA targeting indoleamine 2,3-dioxygenase 1 (IDO1) into a Zinc 2-methylimidazole (ZIF-8)-based nano-metal-organic framework, followed by a coating with GAM membrane. The tumor-homing activity of the GAM membrane facilitated the THINR targeting of the remaining infiltrating tumor cells post-surgical resection. Moreover, activated T cells were recruited to the surgical site via CXCL10-CXCR3 (CXC motif chemokine receptor 3) axis to induce higher levels of immunogenic cancerous cell death, resulting in tumor recurrence inhibition.

Neutrophil and Dendritic Cell-mediated Delivery

Apart from macrophages, neutrophils also show remarkable tumor tropism with the ability to penetrate inflamed brain tumors. Proinflammatory cytokines like interleukin-8 (IL8) and TNFα are known to direct neutrophil migration and are commonly upregulated in the postoperative brain. Nanoparticle-loaded neutrophils can thus be recruited to the inflammatory site and release the cargo through NETosis. This process entails bursting out net-like intracellular structures comprising DNA and protein when activated by cytokine signals in the surrounding environment.[18] The Zhang group adopted such a method to construct paclitaxel (PTX)-encapsulated liposomes, formulated by soy phosphatidylcholine (SPC), cholesterol, and $HG2C_{18}$. These were carried and delivered by neutrophils trafficked towards the inflammatory signals released from the surgical site of the brain.[19] They demonstrated that the neutrophil-mediated nanoparticle delivery effectively penetrates across endothelial cells and brain parenchyma cells, energetically releasing PTX to the remaining invading GBM cells post-tumor resection. The capability of the method to overcome multiple biological barriers, respond to inflammatory factors, and stimulate drug release, enabled a precision GBM-specific chemotherapy through intravenous injection, and resulted in a dramatic inhibition of tumor recurrence post-surgery.

Furthermore, the fundamental role that dendritic cells (DCs) play in antitumor immunity makes these cells another ideal candidate for tumor-targeted nanoparticle delivery. The research findings from Chen et al. highlighted the dual role of DCs when they were used to deliver Dox-loaded nanodiamonds.[20] The polyglycerol-coated nanodiamonds were decorated with a cyclic RGD peptide (tripeptides of L-arginine, glycine, and L-aspartic acid), a GBM-targeting ligand with high binding affinity to the overexpressed integrin αvβ3 receptor. The chemotherapeutic payload, Dox, loaded in the nanodiamonds, is known to induce tumor cell cytotoxicity and the emission of damage-associated molecular patterns (DAMPs). They demonstrated that DCs efficiently infiltrated the GBM and released Dox to tumor cells. Subsequently, the Dox-induced immunogenic GBM cell death activated the carrier DCs, activating lymphocytes downstream via stimulating tumor-derived antigen presentation.

Conclusion

The unmet clinical needs in treating patients with brain malignancy have highlighted the urgency of developing novel antitumor therapeutic modalities. Although patients with certain types of cancers have benefited from the emerging immunotherapy strategies, such progress has yet to be experienced by GBM patients. Recent research findings have revealed the vital role that TAMCs play in inducing GBM immunosuppression, progression, metastasis, and therapy resistance. However, targeted therapy for this predominant population of immune cells in GBM remains understudied to date. Compelling preclinical and clinical studies have identified therapeutic modulation of immunosuppressive TAMCs as a promising new branch to potentiate the anti-GBM immunity and thus improve the therapeutic effects of both immunotherapy and conventional standard treatments. Thanks to the well-documented functionality, versatility, and feasibility, nanotechnology has emerged as a powerful toolbox to enable and improve a wide range of innovative therapeutic strategies; from eliminating immunosuppressive TAMCs to reeducating these myeloid cells to be "good" immune cells or harnessing them as cellular "Trojan horses" for GBM-targeted delivery. Manufactured by rationally designed multifunctional materials, TAMC-targeted nanoparticles have demonstrated their ability to specifically target and effectively modulate TAMCs, either through the pharmacological activity of payload therapeutics or the biological functions exerted by nanoparticles themselves. Undoubtedly, nanotechnology will continuously and significantly propel cancer therapy advances and hold great hope as a promising treatment option for GBM patients.

Acknowledgments

This work was supported by NIH/NCI grant (R01CA266487) to P.Z., NCI Outstanding Investigator Award (R35CA197725) and NIH grants (P50CA221747, R01NS115955) to M.S.L.

References

(1) Thorsson, V.; Gibbs, D. L.; Brown, S. D.; Wolf, D.; Bortone, D. S.; Ou Yang, T.H.; et al. *Immunity* **2018**, *48* (4), 812–30.
(2) (2) Friebel, E.; Kapolou, K.; Unger, S.; Nunez, N. G.; Utz, S.; Rushing, E. J.; et al. *Cell* **2020**, *181* (7), 1626–1642.
(3) (3) Klemm, F.; Maas, R. R.; Bowman, R.L.; Kornete, M.; Soukup, K.; Nassiri, S.; et al. *Cell* **2020**, *181* (7):1643–60.
(4) Quail, D.F.; Joyce, J. A. *Cancer Cell* **2017**, *31* (3),326–41.
(5) Zhang, F.; Parayath, N. N.; Ene, C. I.; Stephan, S. B.; Koehne, A. L.; Coon, M. E.; et al. *Nat Commun.* **2019**, *10* (1), 3974.
(6) Gao, X. H.; Li, S.; Ding, F.; Liu, X. L.; Wu, Y. J.; Li, J.; et al. *Adv. Mater.* **2021**, *33* (9), e2006116.
(7) Conde, J.; Bao, C.; Tan, Y.; Cui, D., Edelman, E. R.; Azevedo, H. S.; et al. *Adv. Funct. Mater.* **2015**, *25* (27),4183–94.
(8) Zhang, P.; Miska, J.; Lee-Chang, C.; Rashidi, A.; Panek, W. K.; An, S. J.; et al. *P. Natl. Acad. Sci. U.S.A.* **2019**, *116* (47), 23714–23.
(9) Zheng, Z.; Zhang, J.; Jiang, J.; He, Y.; Zhang, W.; Mo, X.; et al. *J. Immunother. Cancer.* **2020**, *8* (2), e000207.
(10) Mitchell, M. J.; Billingsley, M. M.; Haley, R. M.; Wechsler, M. E.; Peppas, N. A.; Langer, R. *Nat. Rev. Drug Discov.* **2021**, *20* (2), 101–124.
(11) Paunovska, K.; Loughrey, D.; Dahlman, J. E. *Nat. Rev. Genet.* **2022**, *23*, 265–280.
(12) Zhang, P.; Xu, J. N.; Gao, S. E.; Li, S. Dual-function nanocarriers with interfacial drug-interactive motifs for improved delivery of chemotherapeutic agents. *Nanobiomaterials in Cancer Therapy: Applications of Nanobiomaterials*. Elsevier, 2016; 367–394.
(13) Wu, C.; Muroski, M. E.; Miska, J.; Lee-Chang, C.; Shen, Y.; Rashidi, A., et al. *Nanomed.* **2019**, 16, 126–37.
(14) Deeken, J. F.; Loscher, W. *Clin. Cancer Res.* **2007**, *13* (6):1663–74.

(15) Zhang, W.; Wang, M.; Tang, W.; Wen, R.; Zhou, S.; Lee, C.; et al. *Adv. Mater.* **2018**, *30* (50), e1805557.
(16) Pang, L.; Zhu, Y.; Qin, J.; Zhao, W.; Wang, J. *Drug Deliv.* **2018**, *25* (1), 1922–31.
(17) Zhang, J.; Chen, C.; Li, A. N.; Jing, WQ, Sun P, Huang XY, et al. *Nat. Nanotechnol.* **2021**, *16* (5), 538–548.
(18) Masucci, M. T.; Minopoli, M.; Del Vecchio, S.; Carriero, M. V. *Front Immunol.* **2020**, *11*, 1749.
(19) Xue, J.; Zhao, Z.; Zhang, L.; Xue, L.; Shen, S.; Wen, Y.; et al. *Nat Nanotechnol.* **2017**, *12* (7), 692–700.
(20) Li, T. F.; Li, K.; Zhang, Q.; Wang, C.; Yue, Y.; Chen, Z.; et al. *Biomaterials* **2018**, *181*, 35–52.

PLGA Nanoparticles and Microspheres

Name	Form	Average Diameter	Cat. No
PLGA microspheres	pellets	1 µm	**LG1000-50MG-A**
	powder	2 µm	**805130-50MG**
	pellets	5 µm	**LG5000-50MG-A**
	pellets	10 µm	**LG10K-50MG-A**
	pellets	20 µm	**LG20K-50MG-A**
	powder	25 µm	**805114-50MG**
	pellets	30 µm	**LG30K-50MG-A**
	pellets	40 µm	**LG40K-50MG-A**
	powder	50 µm	**805122-50MG**
PLGA nanoparticles	powder	100 nm	**805092-50MG**
	powder	500 nm	**805149-50MG**

Fluorescent PLGA Nanoparticles and Microspheres

Name	Excitation/Emission	Average Diameter	Cat. No.
Near-IR Fluorescent PLGA microspheres	780/820 nm	1 µm	**LGFN1000-50MG-A**
	780/820 nm	2 µm	**LGFN2000-50MG-A**
	780/820 nm	5 µm	**LGFN5000-50MG-A**
	780/820 nm	10 µm	**LGFN10K-50MG-A**
	780/820 nm	20 µm	**LGFN20K-50MG-A**
	780/820 nm	30 µm	**LGFN30K-50MG-A**
	780/820 nm	40 µm	**LGFN40K-50MG-A**
Near-IR Fluorescent PLGA nanoparticles	780/820 nm	100 nm	**LGFN100-50MG-A**
	780/820 nm	200 nm	**LGFN200-50MG-A**
	780/820 nm	500 nm	**LGFN500-50MG-A**
Red Fluorescent PLGA microspheres	647/670 nm	1 µm	**LGFR1000-50MG-A**
	647/670 nm	10 µm	**LGFR10K-50MG-A**
	647/670 nm	20 µm	**LGFR20K-50MG-A**
	647/670 nm	50 µm	**LGFR50K-50MG-A**
Red Fluorescent PLGA nanoparticles	647/670 nm	100 nm	**LGFR100-50MG-A**
	647/670 nm	200 nm	**LGFR200-50MG-A**
	647/670 nm	500 nm	**LGFR500-50MG-A**
Orange Fluorescent PLGA microspheres	530/582 nm	1 µm	**LGFO1000-50MG-A**
	530/582 nm	10 µm	**LGFO10K-50MG-A**
	530/582 nm	20 µm	**LGFO20K-50MG-A**
	530/582 nm	50 µm	**LGFO50K-50MG-A**
Orange Fluorescent PLGA nanoparticles	530/582 nm	100 nm	**LGFO100-50MG-A**
	530/582 nm	200 nm	**LGFO200-50MG-A**
Green Fluorescent PLGA microspheres	460/500 nm	1 µm	**LGFG1000-50MG-A**
	460/500 nm	2 µm	**805181-50MG**
	460/500 nm	5 µm	**LGFG10K-50MG-A**
	460/500 nm	20 µm	**LGFG20K-50MG-A**
	460/500 nm	25 µm	**805173-50MG**
	460/500 nm	30 µm	**LGFG30K-50MG-A**
	460/500 nm	40 µm	**LGFG40K-50MG-A**
	460/500 nm	50 µm	**805165-50MG**
Green Fluorescent PLGA nanoparticles	460/500 nm	100 nm	**805157-50MG**
	460/500 nm	200 nm	**805211-50MG**
	460/500 nm	500 nm	**805300-50MG**

Polycaprolactone (PCL) Nanoparticles and Microspheres

Name	Form	Molecular Weight (M_w)	Average Diameter	Cat. No.
PCL Microparticles	10 mg/ml suspension in DI water	14,000	1 µm	**PCL1000-5ML-A**
	10 mg/ml suspension in DI water	14,000	2 µm	**PCL2000-5ML-A**
	10 mg/ml suspension in DI water	14,000	5 µm	**PCL5000-5ML-A**
	10 mg/ml suspension in DI water	14,000	10 µm	**PCL10K-5ML-A**
	powder	14,000	20 µm	**PCL20K-50MG**
	powder	14,000	30 µm	**PCL30K-50MG**
	powder	14,000	50 µm	**PCL50K-50MG**
PCL Nanoparticles	10 mg/ml suspension in DI water	14,000	100 nm	**PCL100-5ML-A**
	powder	30,000	200 nm	**805106-50MG**
	10 mg/ml suspension in DI water	14,000	200 nm	**PCL200-5ML-A**
	10 mg/ml suspension in DI water	14,000	500 nm	**PCL500-5ML-A**

MERCK

The Future of Drug Delivery

Ready-to-use preformulated lyophilized liposomes

Liposomes are one of the most common drug delivery carriers for small molecules and nucleic acid therapeutics.

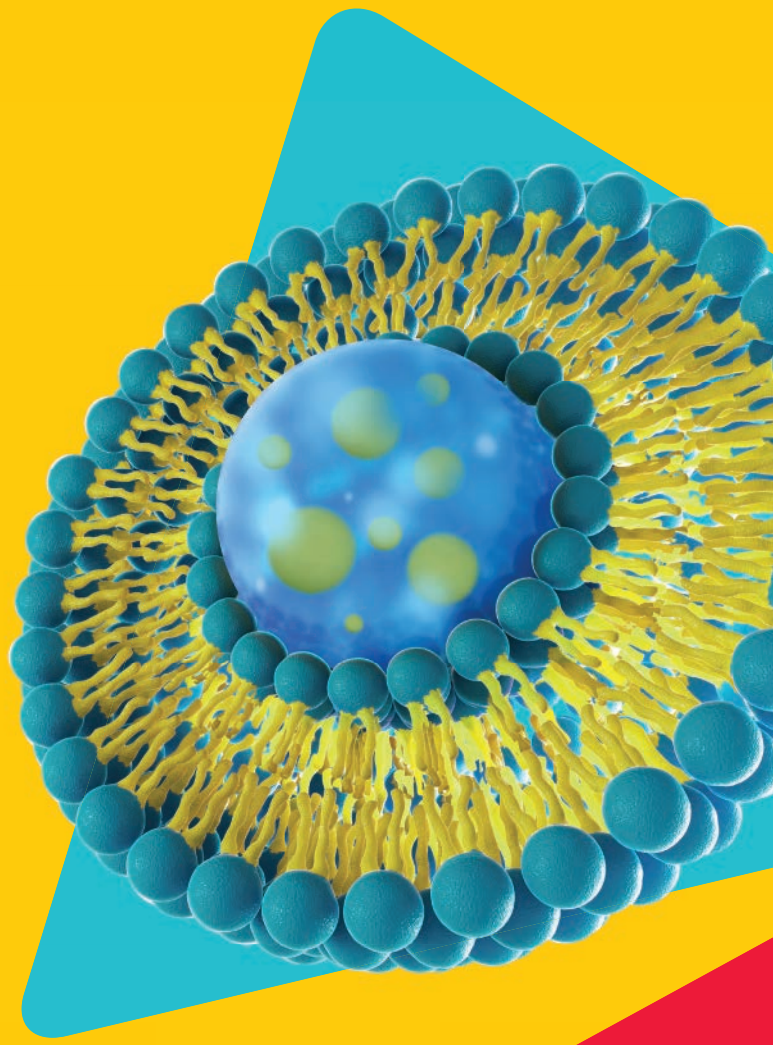

We offer a variety of preformulated liposomes including:

- Cationic liposomes
- Natural liposomes
- PEGylate liposomes

Upon hydration of the lyophilized formulation, the liposomes are formed and ready to use.

For a complete list of preformulated lyophilized liposomes visit:
SigmaAldrich.com/liposomes

43539 08/2022

The Life Science business of Merck operates as MilliporeSigma in the U.S. and Canada.

Sigma-Aldrich®
Lab & Production Materials

Merck KGaA
Frankfurter Strasse 250
64293 Darmstadt, Germany

MID-CAREER RESEARCHER AWARD

The Material Research Society presents the Mid-Career Research Award to recognize exceptional achievements in material research made by mid-career professionals. Merck is proud to endow this award.

Molly Stevens

Molly Stevens

Affiliation: Imperial College London, UK

For innovative biosensing nanomaterials technologies for point-of-care disease diagnostics

Prof Molly M Stevens FREng FRS is Professor of Biomedical Materials and Regenerative Medicine and the Research Director for Biomedical Material Sciences in the Department of Materials, in the Department of Bioengineering and the Institute of Biomedical Engineering at Imperial College London.

Molly's multidisciplinary research balances the investigation of fundamental science with the development of technology to address some of the major healthcare challenges. Her work has been instrumental in elucidating the bio-material interfaces leading to the creation of a broad portfolio of designer biomaterials for applications in disease diagnostics and advanced therapeutics. Her substantial body of work influences research groups around the world (>400 publications, h-index 100, >39k citations, 2018 and 2021 Clarivate Analytics Highly Cited Researcher in Cross-Field research).

Molly holds numerous leadership positions including Director of the UK Regenerative Medicine Platform "Smart Acellular Materials" Hub, Deputy Director of the EPSRC IRC in Early-Warning Sensing Systems for Infectious Diseases and Scientist Trustee of the National Gallery. She is Fellow of the Royal Society and the Royal Academy of Engineering (UK), Foreign Member of the National Academy of Engineering (USA) and International Honorary Member of the American Academy of Arts and Sciences.

Lit. No. MK_BR9817EN